UNIVERSITÄT PADERBORN

# Application of Principle Component Analysis to STEM based EELS and EDX data cubes 2019.

***JULY 8***

Nanopatterning - Nano analysis - Photonic Materials
Authored by: VSR Bala Krishna Potla
Department of Materials Science
Universität Paderborn - Germany

Nanophotonics & Nanomaterials

# Author Note

*This Project is performed as a part of Master's degree in Materials Science academic curriculum course at Universität Paderborn in Germany. This project is done in semester -3 with the working group of 'Nanopatterning - Nano analysis - Photonic materials' under the supervision of Professor. Doctorate. Jörg Lindner with coordinator Mr. Vinay Kunnathully sathees Kumar (Ph.D.) from Physics department. I thank to Prof. Lindner for theoretical support and explanation of EELS concepts and Vinay for technical assistance regarding evaluation and understanding spectrums of specimens.*

*With Regards*

*VSR Bala Krishna Potla.*

# Contents

# Application of Principle Component Analysis to Electron Energy Loss Spectroscopy and Energy dispersive spectroscopy Data.

Universität Paderborn , Materials Science, Paderborn, Germany-2019.

A R T I C L E  I N F O

*Article history :*
This project is done as a part of Master's course in Materials Science project curriculum at Universität Paderborn, Germany in 2019.

***KEYWORDS :*** [ STEM & TEM, EELS, EDX, PCA, Scatter plot, Noise, Clustering.]

A B S T R A C T

Principle component analysis(PCA) is one of the multi statistical analysis technique applied for investigating STEM (scanning transmission electron microscope) spectrum images(SI). Application of PCA for STEM atomic column 'Electron energy loss spectroscopy' (EELS) and 'Energy dispersive spectroscopy'(EDS) image data sets reduces the random noise efficiently and gives the fingerprint of material characterization in terms of bonding state, electronic structure, chemical state, identification of elements with good spatial atomic resolution. In this project we investigate PCA math for representing EELS and EDS image data sets from high noise to noise reduction image sets with spectrum indication of elemental characterization.

---

## 1 Introduction

Material characterization with elemental mapping of spectral analysis is highly desirable in the STEM and electron based spectroscopy fields especially EDX and EELS provided spatially resolved spectroscopic data in spectrum Images(SI) with large sets of spectra generated as electron probe is scanned in rastered format across the specimen ending in the result as 2D spectral map up to sub-Angstrom or nanometers scale resolution which is stored in a data cube which will be discussed in eels part.. Development in aberration correlated electron spectrospy typically eels' experiments consists of huge spectra which is limited to the specimen drift, number of scans points, signal -to-noise ratio depends upon total acquisition of time and amount of signal intensity. Improvement in aberration corrected microscopes with high brightness guns, the limitation has shifted from detection method towards the sample. Due to high beam voltage focused on specimen in raster format there is a possibility of sample damage and hence exposure of specimen is limited to a few seconds and often limited to beam voltage. Technological advancement in stem and eels equipment has increased the stability in terms of specimen drift, electromagnetic condenser's and faster acquisition facilitates the ability to collect huge set of spectra in data cube. Generally, eels data cube consists of 100 × 100 pixels and a CCD spectrometer range of 2048 bins. Due to increase in bulk data cubes within less time(minutes),

demand for appropriate statistical analysis of spectrums, background correction, noise redundancy is strategic, which can be investigated by 'principle component analysis'. PCA is an optical algorithm which provides the least number of orthogonal vectors requires to capture a given percentage of image variance. The eels data consists of gaussian and poissionian noise filtered by PCA.

## 1.1 Light -Matter Interactions

The fundamental physics of any electron based spectroscopy is 'Interaction of light (electrons) with matter', when a beam of specific energy range hits the specimen it excites radiation as per Planck's radiation law which gives the concept of Ionization radiation which is not a single technique but a diversity of different ones that offer unique possibilities to gain insights into structure, topology, morphology and composition of a material. Different types of imaging and spectroscopic techniques represent indispensable platforms for testing all kinds of materials in a smaller size scale within the limit of single atomic scale. Specimens of inorganic and organic materials, micro and nano structures, minerals and biological objects can be subjected to electron microscopy for analysis. When a fast moving beam of electrons hits the material, the atoms gets excited and electrons gets transferred from k, L, M, N shells and there by producing a wide range signals shown in Figure 1. Each signal has a specific content of material hidden information which can be extracted by using different electron based spectroscopy techniques such as AEM, XEDS, XPS, EELS, TEM….etc. As there is a wide range of applications of light with matter here, we get insight about STEM based EELS and EDS data . Electron matter or beam of light incident on specimen is classified into two types which are elastic and inelastic interactions. In elastic interaction no transfer of energy from electrons to specimen which results the electron leaving the sample has its original energy $E_0$ [1]

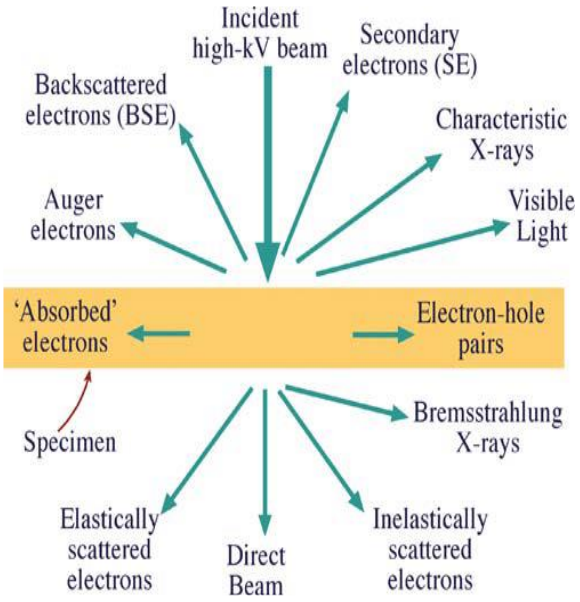


***Figure 1 Interaction of light with matter** [1]*

$$E_{el} = E_0$$

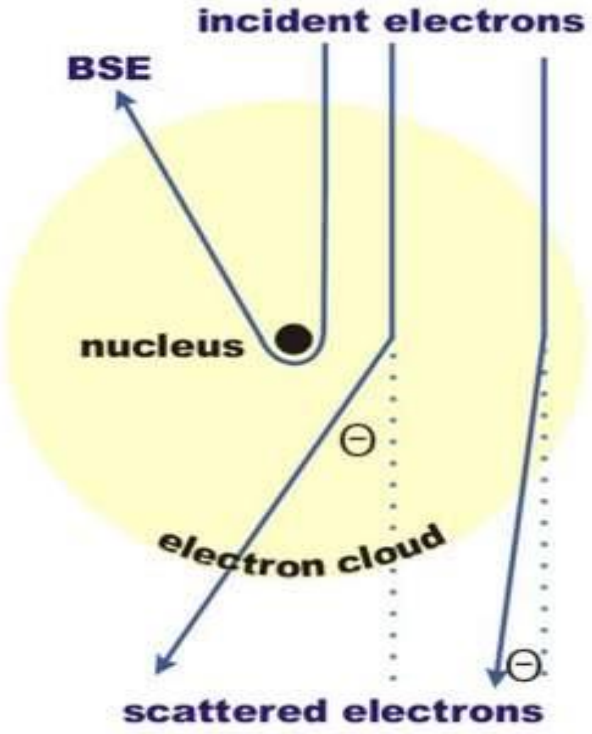


***Figure 2 Scattering of electron inside electron cloud of an atom** [1]*

From figure 1 we can see beam passing through specimen without any energy loss projected as direct beam. Elastic scattering occurs when electrons are deflected from its path due to coulomb interaction with the positive potential developed inside the electron cloud there by primary electrons loses no energy or a less amount energy which is not considered. These signals are mostly analyzed in TEM and other diffraction methods mostly. Electron penetrating into the electron cloud of an atom is attracted by the positive potential of the nucleus due to electrostatic

or coulombic interactions and its path is deviated towards the core shown in figure 2 and coulombic force is stated as in (1) but here in this project our technique is related to inelastic interaction based [2]

$$F = Q_1 Q_2 / 4\pi\varepsilon_0 r^2 \ldots\ldots\ldots\ldots\ldots\ldots\ldots (1)$$

## 1.2 Inelastic Interaction

In Inelastic interaction energy is transferred from the electrons to sample thereby causing loss of electron energy when interacted.

$$E_{el} < E_0$$

Energy transferred to specimen causes several signals such as

**a)** Inner -shell ionization : In the process of ionization it takes "Excitation, Relaxation and

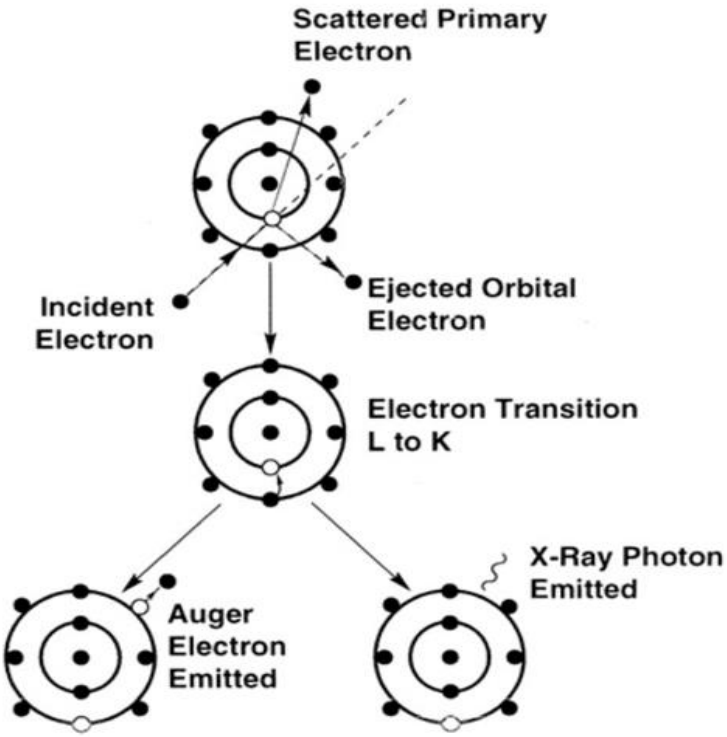


***Figure 3 Mechanism of inelastic scattered electron inner ionization process of excitation, relaxation, emission*** *[2].*

Emission". From figure 3, When an incident electron or STEM beam passes through the pack of electrons around an atom the electrons gets excited with transfer of energy towards in any area of the surrounding atom's electron shells. When the transfer of energy to electron is reached to threshold energy level limit, electron is promoted to the lowest unoccupied electron level. If the transferred energy is sufficient to eject the electron into the vacuum, atom gets ionized because of its positive charge carrier. In this state, energy transfer to an electron of an inner shell is crucial due to resulting electronic state of the generated ion is energetically unstable. An inner shell with a low energy has an electron vacancy as compared to higher energy levels are occupied state again, an electron travels from higher level to low level to fill vacancy position and by this whole process, the atom gets realaxed and the excess energy of electron is emitted out, which dropped to a lower state corresponds to the diffrence between the energy levels. In this difference of energy levels X-rays, auger electrons are also generated but, as of this project we deal with characteristic electron energy loss released when electron gets relaxed and excess is released resulting "Electron energy loss" which became the base for investigating chemical nature, elemental identification and mapping with the

invention of "Electron energy loss spectroscopy" and also 'energydispersive spectroscopy' in contrast [2].

From figure 4 we can see the generation of X-ray, when an electron from a higher energy level drops to fill the electron hole in a lower level, the difference energy is emitted as high energetic electro-magnetic radiation. In the initial stage ionization energy is transferred from an incident electron to an electron in an inner shell of an atom which results the electron gets excited and ejected to high energy orbital levels as a result vacancy in the low energy level in K-shell. In the second stage electron from higher energy level ($L_3$) level drops to K-shell and fills the vacant position of low level. And when this happens the surplus difference energy is emitted as an X-ray quantum with a characteristic energy. From figure 5 we look through the possible electron transitions generating X-rays. Electron holes might be generated in all electronic states from K to L in fig 5. Electron hole in K-shell is filled by an electron from L or M shells respectively leading to Kα or Kβ radiation. Similarly, vacancy in the L shell is filled by an electron from M shell generating Lα radiation. If more electrons with energy levels high, then more transitions within the shells are possible. It is also noteworthy that energy difference between the M and K shells is greater than L and K shells. According to Bohr's atomic model different transitions appear from different various energy levels whereas, the actual energy level depends upon the hybridization of an atom. To understand the theory of

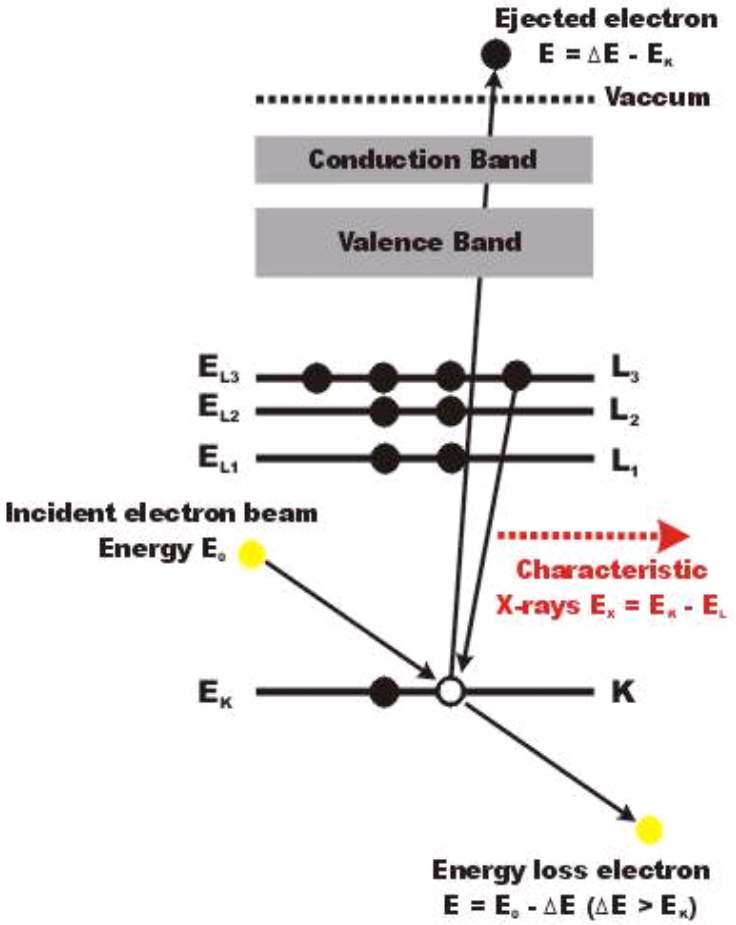


*Figure 4 Generation of characteristic X-ray quantum. Ionization energy initiated with transfer of incident electron within electron cloud [2]*

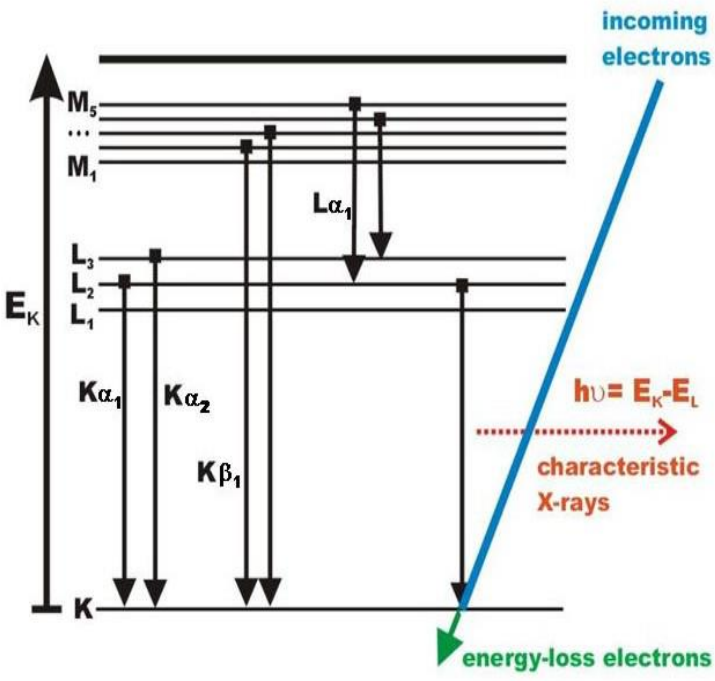


*Figure 5 Electron transitions generating X-rays and transfer of electron from higher energy shells to lower shells [2].*

ionization, we consider 'titanium' here from a perovskite type of strontium titanite (**$SrTio_3$**) nano cube which were synthesized by using a hydrothermal process and the thin films of these nano cubes were deposited on an n-type silicon wafer by using spin coating technique and **$SrTio_3$** nano cubes were characterized by using STEM along with EDS. From figure 6 we look at the X-rays generation and electronic configuration as [$1s^2$ $2s^2$ $2p^6$ $3s^2$ $3p^6$ $4s^2$ $3d^2$] and transitions are K shell--filled by 2p, 3p levels corresponding Kα, Kβ radiation and one in 2s state from 3p level corresponding to L radiation and similarly further transitions involve in the 2p or 3p state [1] [2].

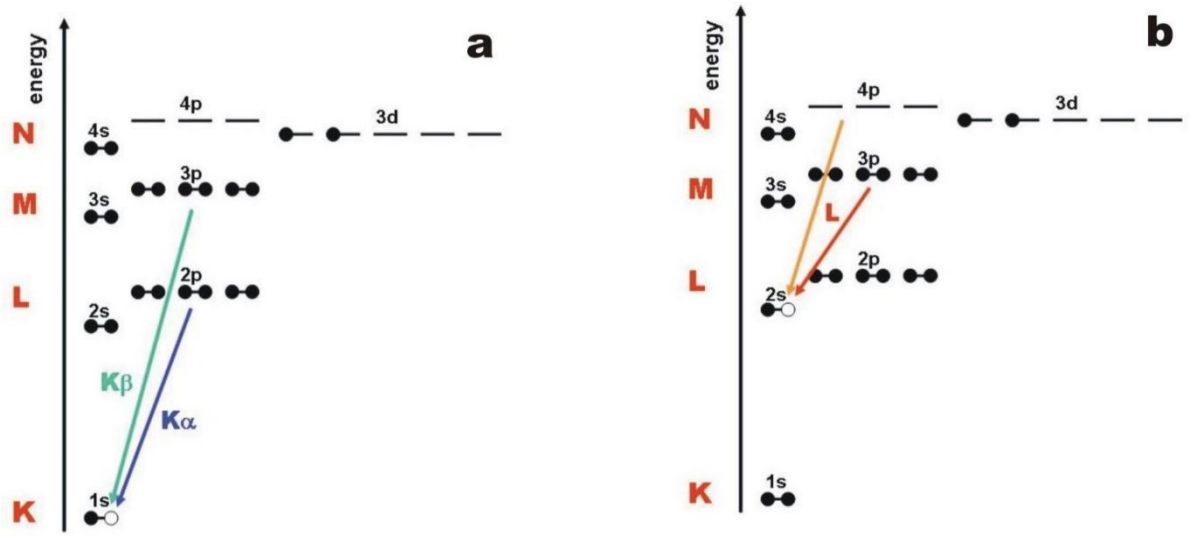


***Figure 6 Possible Ionizations in the K shell (a) and L shell (b) with electron transitions in titanium** [2].*

**b)** Bremsstrahlung or Braking radiation : Electron passing an atom within its electron cloud is decelerated with the effect of coulomb force of nucleus. This inelastic interaction emits X-rays that can carry any amount of energy up to that of the incident beam **$E \leq E_0$**. Braking radiation is the main factor that contributes continuous background factor in X-ray spectrum. Only X-rays with low energy up to **100 eV** are absorbed by the sample and cannot observed in the X-ray spectrum. The background of the spectrum is mostly bremsstrahlung.

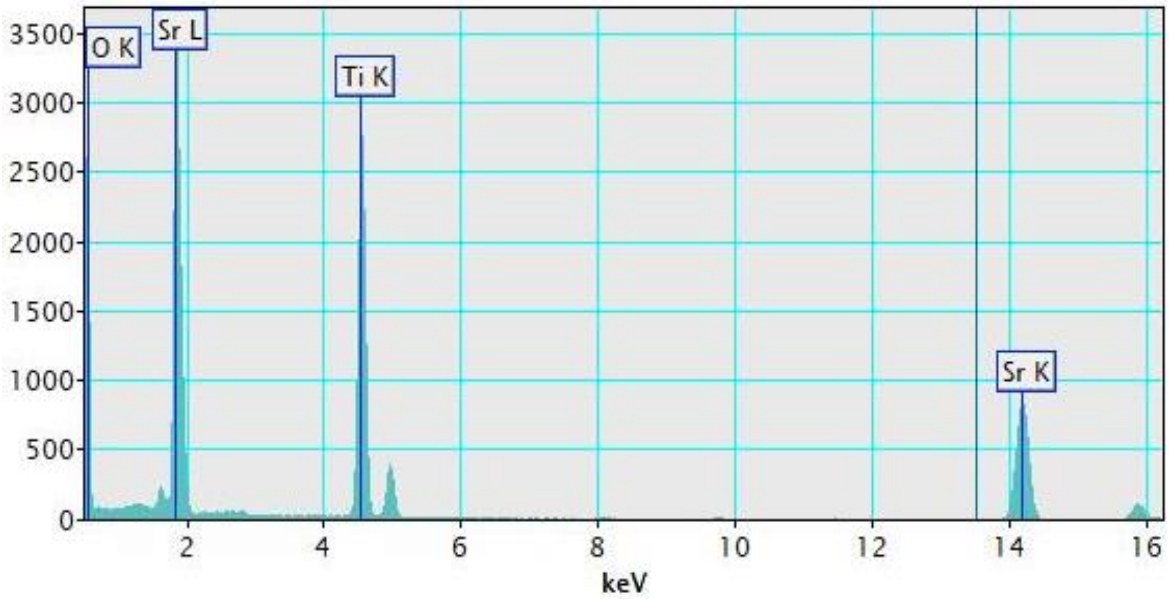


***Figure 7 $SrTio_3$ EDX spectrum generated through PCA plugin***

**c)** Secondary electrons : SEs are ejected from conduction or valence bands of the atom in the specimen within the energy range of $\leq$ **50eV**. If the electrons are ejected from an inner shell by the energy released when, an ionized atom returns to the ground state then these SEs are called Auger electrons. SEs are free electrons which are not associated with a specific atom which results without any specific elemental information and SEs are also weak they can only escape if they are near to the specimen surface. SEs are used in SEM for image formation of specimen surface and also in STEM where they provide high resolution and topographic images of specimen surface [1] [2].

**d)** Phonons : Phonons are collective oscillations of the atoms in a crystal lattice and can be initiated by an up-take of energy from the electron beam. When an incident electron (beam) hits an atom transfer of energy occurs and this leads to vibration of atom since, all atoms are connected together in a crystal lattice , the vibration of an atom is felt by others that also starts to vibrate. Due to this process , the absorbed energy is distributed over a large volume and the resulting collective vibrations are equivalent to heating up the specimen. Phonons are generated as by product with any inelastic electron matter interaction. Phonons can be controlled by effective way of cooling specimen [1].

**e)** Plasmons : Plasmons are collective oscillations of free electrons that occur when a beam electron interacts with the free electron gas. From Electrons in a metal acts as a gas free electrons. The free electron gas electrons are repelled initially by passing the electron, within the limits imposed by the solid. In plasmon scattering the fast electron excites a ripple in the plasma of free electrons in the solid and the energy of plasmon depends only on the volume concentration of free electrons n in the solid and it is given by

$$Ep = D\,[ne^2/m]^{1/2} \quad \ldots\ldots\ldots(2)$$

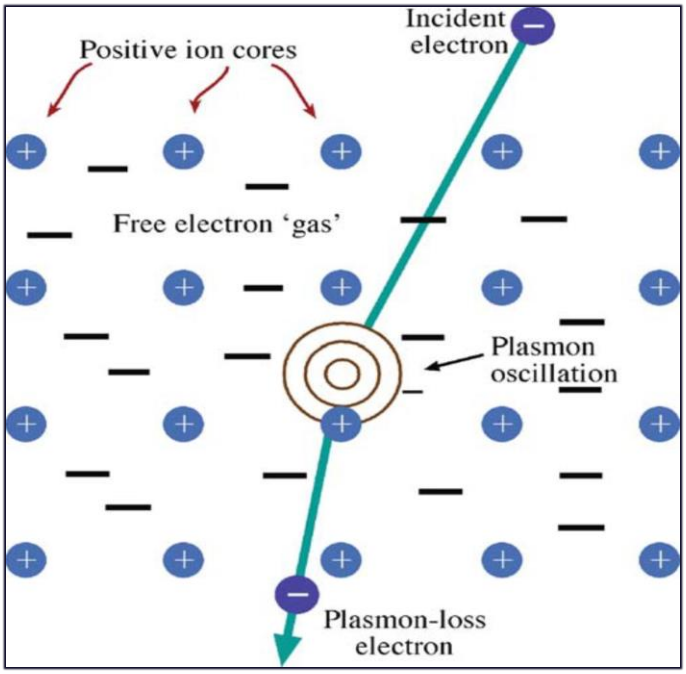


***Figure 8 Schematic view of a high energy beam electron exciting plasmon oscillation in a free electron gas that penetrates the ion cores in a metal [1].***

Typically, $E_p$ is the energy loss suffered by the fast electron is similarly 15eV and the scattering intensity /unit solid angle which has an annular width given by $\boldsymbol{\Theta_E = Ep/2E_0}$, where $E_0$ is incident of voltage and $\boldsymbol{\Theta_E}$ is similar to $10^{-4}$ radian. The energy of plasmon is converted into atom vibrations and the mean free path for plasmon excitation is small in between 50-150 nm. Plasmons play important role in EEL spectra as plasmons has the highest valence electrons it plays sensitivity in chemical analysis [1].

**f)** Cathodoluminescence : When a semiconductor is hit by an electron beam, electron-hole pairs are generated . When an energy of incident electron is transferred to the electron in valence band it is promoted to conduction band and the resultant is so called electron hole pair. This exited state of the semiconductor is energetically instable, and the material can relax by filling this electron hole by an electron dropping down from the conduction band and this process is designated as recombination which leads to the emission of a photon carrying the difference energy $\mathbf{E=h\nu}$ and this energy corresponds to that of the band gap which is used to measure band gap energy of semiconductors [2].

## 2 Introduction of STEM

The notion of the electron based STEM/TEM microscopes is to study atomic configurations of elements in different compositions and to project the whole structure of atoms arrangement as image which is visible to human eye by using the wave nature of electrons and the combination of convex lenses, electromagnetic fields mechanisms. The wavelength of a free electron's energy-momentum conservation is derived from special relativity theory and the de Broglie relation which is the basic idea of understanding wave particle duality:

$$E_{tot}^2 = p^2c^2 + m_0^2c^4 \ldots\ldots\ldots\ldots\ldots\ldots\ldots\ldots\ldots(3)$$

$$\lambda = h/p \ldots\ldots\ldots\ldots\ldots\ldots\ldots\ldots\ldots\ldots\ldots\ldots\ldots\ldots(4)$$

$E_{tot}$ is the total energy of the system, $c$ is the velocity of light, $h$ is the Planck constant, $p$ is the relativistic momentum and $m_o$ is the rest mass of an electron. The wavelength of the electron as the de Broglie wavelength is given as:

$$\lambda = h/\sqrt{2m_0eE\left(1+\frac{eE}{2m_0c^2}\right)} \ldots\ldots\ldots\ldots\ldots(5)$$

$E$ is the accelerating potential energy of STEM/TEM, and e is the absolute value of electron charge(e= $1.6*10^{-19}$ coulomb) and the particle nature of an electron is the basis for the design of electron guns, electromagnetic lenses, deflectors. The basic equation is the relativistic ally modified Newton's equation:

$$dp/dt = [(-e)E + (-e)\upsilon \times B \ldots\ldots\ldots\ldots\ldots\ldots\ldots(6)$$

here $\boldsymbol{p}$ is relativistic momentum $m\upsilon = m_0\upsilon$ in the nonrelativistic condition and $\upsilon$ is the velocity of a travelling electron, $E$ is electrostatic field, $B$ is a magnetic field. Interaction between electrons and specimens in an ordinary scattering condition we use the time independent Schrödinger equation as:

$$\nabla^2\psi(\boldsymbol{r}) + \frac{8\pi^2me}{h^2}[E + V(r)]\psi(r) = 0 \ldots.(7)$$

E is the accelerating voltage and v is the electrostatic potential of a specimen [3].

### 2.1 Mechanisms in STEM

From fig. 9 [4] we can see the schematic view of the STEM optical configuration in which an electron source is emitted with varying 30 KV to 300 KV voltage. A series of lenses focusses a beam to form a spot or probe size of 0.08 nm at 200 KV and 0.20 nm at 30 KV which interacts with a thin electron transparent sample and lens are avoided in final focusing sample and other condenser lenses are joined which provides enough demagnification for the electron beam in focusing at the atomic scale. Aberrations of demagnifying lens governs the optical system. An objective aperture is used to restrict its numerical aperture to a size where the aberrations do not lead to a significant blurring of the probe. The objective aperture has two important consequences-it imposes a diffraction limit to the smallest probe diameter that may be formed and electrons that do not pass through the aperture are lost where aperture restricts the amount of beam current available. And scan coils are arranged to scan the sample in a raster format in which different scattered signals are produced, detected and plotted as magnified image which gives the

bulk information of a material. Wide range of signals are generated in the STEM (fig 1) but, we discuss only the possible ones

i. Transmitted electrons that leave the sample at low angles generates 'Bright field' images(BF).
ii. Transmitted electrons that leave the sample at high angles generates annular dark field images(ADF).
iii. Transmitted electrons that have lost a significant amount of energy as they pass through the specimen can be measured by using 'Electron energy loss spectroscopy'(EELS).
iv. X-rays generated from electron excitations in the sample are measured by EDX or XEDS.

Nanometer or sub-nanometer or picometer sized electron probes forms the STEM SI pixel by pixel with a beam convergence of a few tens milliradian by reducing the cross over generated below the electrode of an FEG(field emission gun) by using two or three condenser lens and the pre-field of the objective lens. The probe size is determined by the brightness of electron gun and the aberration of the final converging lens [3].

$$d = \sqrt{\frac{0.4i}{B\alpha^2}} \ \ where\ i = \frac{en_i}{\Delta t} \ldots\ldots\ldots\ldots (8)$$

Where $B$ is the brightness of gun and $\alpha$ is the semi angle of electron convergence, $i$ is the probe current, $\Delta t$ is the recording time per pixel and $n_i$ is the number of electrons per $\Delta t$ and the unit area. The brightness of a thermionic gun at 100KV is in the range of $10^5$ A/cm$^2$sr and FEG is $10^8$ A/cm$^2$sr which makes clearly FEG is crucial for generating brighter and finer electron probe for STEM imaging. The contrast of TEM/STEM images is derived by

$$C = \frac{\Delta n_i}{n_i} = \frac{effective\ signal}{background} \ldots\ldots (9)$$

Here, $n_i$ is the electron count contributing to the image formation of background and $\Delta n_i$ is the image signal determined by scattering phenomena in the specimen and detector efficiency and the incident electrons also obeys passion distribution and have a fluctuation of $\Delta N = \sqrt{N}$, N stands for number of electrons and the quantity $\Delta n_i > 5\ \Delta N$.

As per rose's condition ($\Delta n_i > 5\sqrt{N} = 5\sqrt{n_i}$) and hence we obtain:

$$C > \frac{5}{\sqrt{n_i}} \ldots\ldots\ldots\ldots\ldots\ldots\ldots\ldots (10)$$

The concept of resolution changes with change in probe size and also a larger $n_i$ is required when image contrast is set [3].

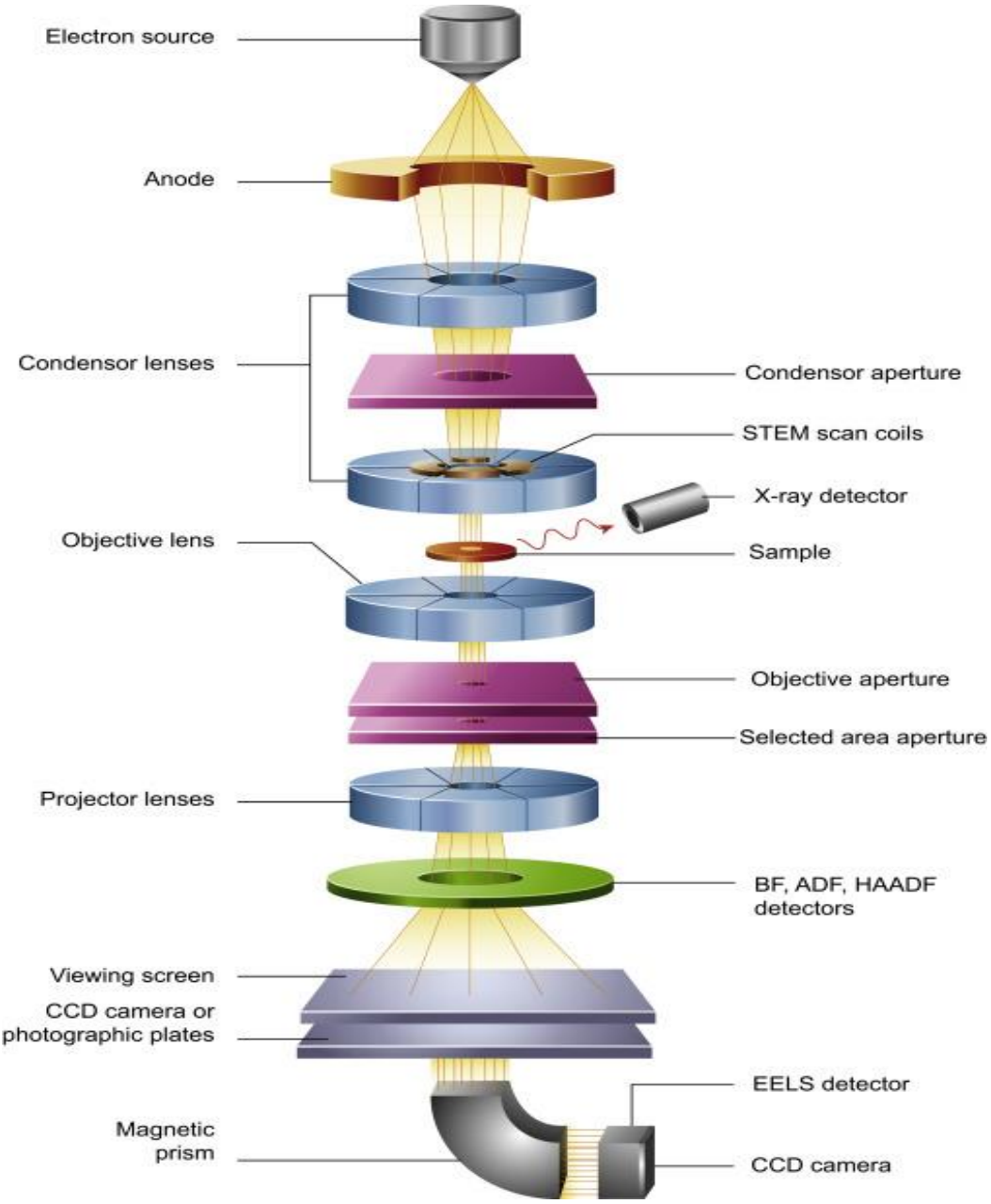


***Figure 9 Schematic view of Mechanisms involved in STEM*** *[4]*

## 2.2 STEM versus TEM

Conventional transmission electron microscope and scanning transmission electron microscope works under the same principle of imaging method by using incident electrons where Fourier transformation takes place through a convex objective lens, intermediate lenses and projector lenses for imaging. From figure 10 we can clearly make the difference in between TEM and STEM optical arrangement and focusing specimen. By making some changes like magnifiers, condenser lenses in TEM it's easier to convert STEM. In STEM mode the specimen is scanned in raster format by each point/line with fine spot probe where as in TEM mode the specimen is scanned all over. STEM has the combined features of SEM and TEM such as:

i. Imaging in a scanning mode similar to the modes of facsimile and televisions.
ii. Specimen can be scanned from upper-left to lower-right pixels of a specimen.
iii. Imaging by electrons transmitted through specimens.
iv. Thin specimens are required for transparent transmission mode.

STEM has the ability to detect single atoms in annular dark field where images are formed using large angle scattered electrons and ADF-STEM images are having resolutions better then TEM. Because of raster format scanning with small probe elemental mapping, electronic structure is easier with EELS and EDX.

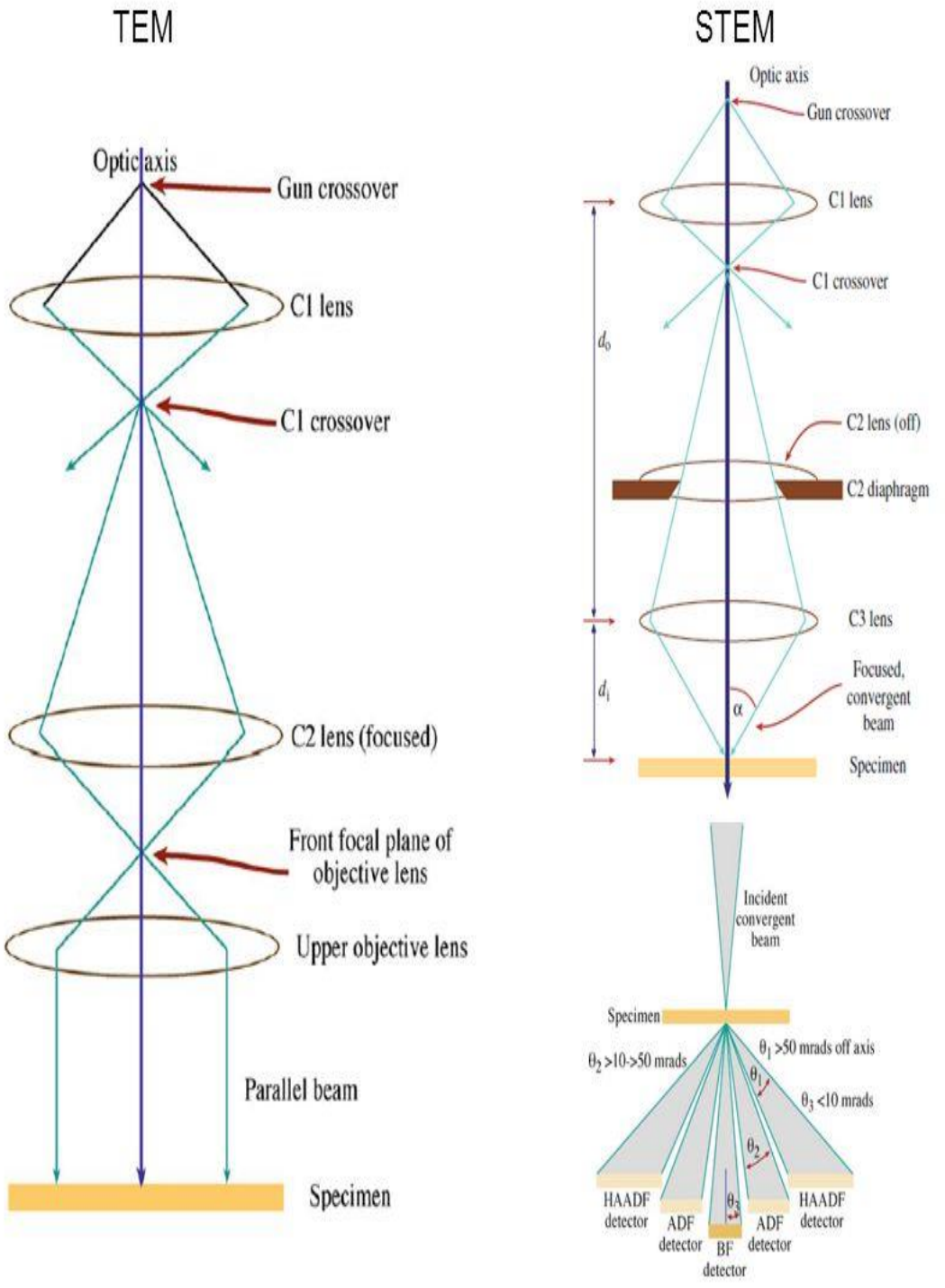


***Figure 10 Basic view of TEM and STEM instrument arrangement of imaging method***

***Figure 11 JEOL -JEM-ARM200F type STEM $C_S$ corrected and EDX attached with Be window at Universität Paderborn.***

***Figure 12 EEL Spectroscopy mounted at the bottom of STEM.***

## 2.3 EELS in STEM

The energy lost by a fast moving electron through its interaction with a specimen generates a different range of signals as discussed in earlier part of 'Interaction of light with matter' with two phenomena of elastic and inelastic based interactions. EELS is one of the inelastic scattering

technique which provides useful information for studying chemical, physical and optical properties of materials. The full potential of EELS work can be extracted when it is combined with the very high spatial resolution furnished by the fast electron in a STEM. In this technique two configurations exist of which one is the beam is fixed and broad in which filtered images are acquired and the other is a focused beam scans a sample and an EELS spectrum is taken at each pixel of the scan which is called 'spectrum imaging'. The parallel acquisition of the elastic and inelastic signals with atomic scale resolution up to sub-nanometer levels helps to investigate elemental mapping, studying the structure of CNT's, and nano objects, fingerprint of materials and identification of elements within the sample. The measurement of inelastic scattering intensity of a fast incident electron as a function of energy loss *ΔE* with probability of differential cross section is given by Fermi 's golden rule [3].

$$\frac{d\sigma}{d\Omega} \propto \frac{k_f}{k_i} \left| \iint \varphi_f^* \exp[2\pi i(k_i - k_f) . r_e] V(r_e, r_a) \varphi_i d^3 r_e d^3 r_a \right|^2 \ldots\ldots (11)$$

$\varphi_f$ and $\varphi_i$ are final and initial states of electrons in a sample, $k_i$ - $k_f$ = q denotes the momentum transfer as hq (h=plank's constant) and dΩ is the partial solid angle. $V(r_e, r_a)$ is the coulomb interaction between an incident electron and an atom with coordinates are $r_e, r_a$. By considering the interaction between a fast incident electron and the electrons of an atom with

$$V = \frac{-e^2}{4\pi\varepsilon_0 \left| r_e - r_a \right|} \ldots\ldots\ldots\ldots\ldots\ldots\ldots\ldots\ldots\ldots\ldots\ldots\ldots\ldots\ldots\ldots (12)$$

From equation 12 the differential cross section becomes:

$$\frac{d\sigma}{d\Omega} \propto \frac{k_f}{k_i} \frac{1}{q^4} \left| \int \varphi_f^* \exp(2\pi i q . r_a) \varphi_i d^3 r_a \right|^2 \ldots\ldots\ldots\ldots\ldots\ldots\ldots (13)$$

Now we introduce Rutherford scattering in the coefficient of equation (13) in a form of $1/q^4$ and the spectral features are determined by the excitations of the electrons in the specimen. The cross section is also written as the following equation using the loss function lm(-1/ε), scattering angle Θ, characteristic angle $\Theta_E$:

$$\frac{d^2\sigma}{d\Omega \Delta E} \propto \frac{1}{\theta^2 + \theta_E^2} \mathrm{lm}\left(\frac{-1}{\varepsilon}\right) \ldots\ldots\ldots\ldots\ldots\ldots\ldots\ldots\ldots\ldots\ldots\ldots (14)$$

Where $k_i = k_f$ and $q^2 = k_i^2(\theta^2 + \theta_E^2)$ and ε is the dielectric function of a specimen. $\Theta_E$ represents the characteristic angle $\theta_E = \Delta E/2E$ and E is the accelerating voltage. Valence electron collective excitation can be observed in the low loss energy range and the dielectric properties of the specimen (ε(ΔE) or ε (ω) can be measured through the loss function from equation (14) where $\Delta E = \bar{h}\omega$. Core electron transition excitations can be observed in the high energy loss range and chemical analysis can be performed through the one-electron approximation and the dipole transition approximation. Core loss signal is observed as an edge shape on a background which is often called k, l, m ,n edge. After background correction core loss intensities can be investigated. A quantitative composition of a specimen can be evaluated using 'Gatan micro suite software' with the ratio of multi core loss intensities. A typical EELS spectrum consists of three regions : zero loss peak(ZLP) at 0 -0.3eV, low loss(LL) at less than 50eV and core loss(CL) obtained at above 50eV of energy range. Core loss spectrum reflects an excitation from a core level to unoccupied states, chemical bonding information such as oxidation and reduction states can be obtained using an energy-loss near edge spectrum (ELINES) and distribution of near neighboring atoms (radial distribution function RDF) extended energy loss fine structure

(EXELFS) which makes advantage of EELS over EDX. EELS is often applied for relatively low atomic number (Z) elements rather than EDX due to the fluorescence yield of X-rays becomes low in low-Z elements, and low energy X-rays emitted from low-Z elements are easily absorbed in the specimen. Element specific intensity is proportional to each partial cross section $\sigma(E, \beta, \Delta)$ Which can be calculated using software application and a few parameters including the collection angle $\beta$ and energy loss range $\Delta$.

1) Zero loss peak : The ZLP is the signature of electrons which do not undergo inelastic scattering or with an elastic interaction in the sample but contains valuable information for calculating specimen thickness and as a result of ZLP which starts at 0eV to 0.3eV and it becomes the starting of EELS spectrum and next peak after it becomes for quantification. Near to ZLP interband transitions occurs which gives about band structure.
2) Low loss region : The low loss region which is less than 50eV consists of highest valence electrons which may be called as VEELS. The plasmon peaks(discussed in 1.2.4) are the predominant feature in LL region and it provides valuable information of the optical and dielectric properties of material. Signal intensities in LL region are higher than HL region.
3) High loss region : The HL region occurs at greater than 50eV which consists of ionization edges called 'Extended line near edge structure' which gives the element oxidation and reduction states. And at the final edge of the EEL spectrum consists EXELFS(extended energy loss fine structure) which gives the information of electrons from the distribution of near neighboring atoms(radial distribution function RDF) [3] [5].

The typical EELS spectrum can be seen in figure 13 and EELS spectrum maximum range is in the order of 2000eV.

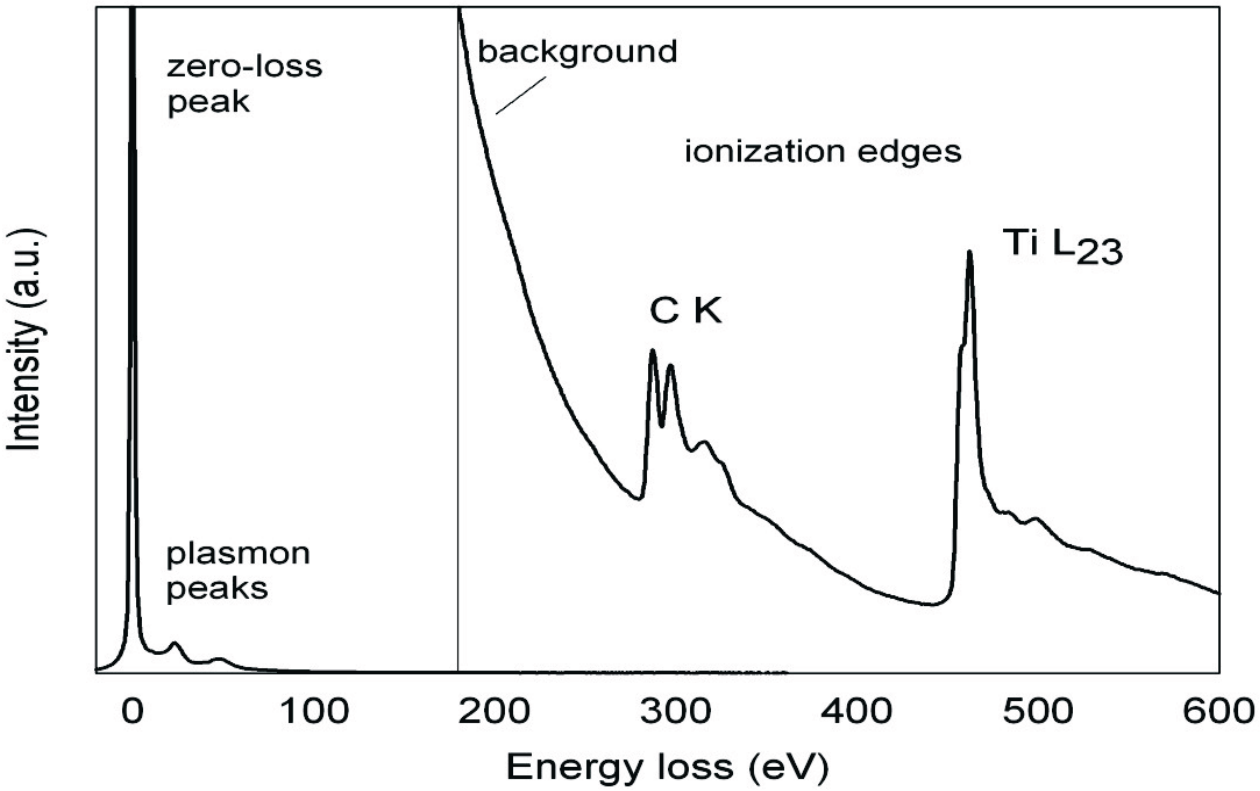


***Figure 13 Typical EELS spectrum of a 20nm thin titanium carbide specimen recorded in CTEM at 200KV equipped with an EFTEM*** *[6]*

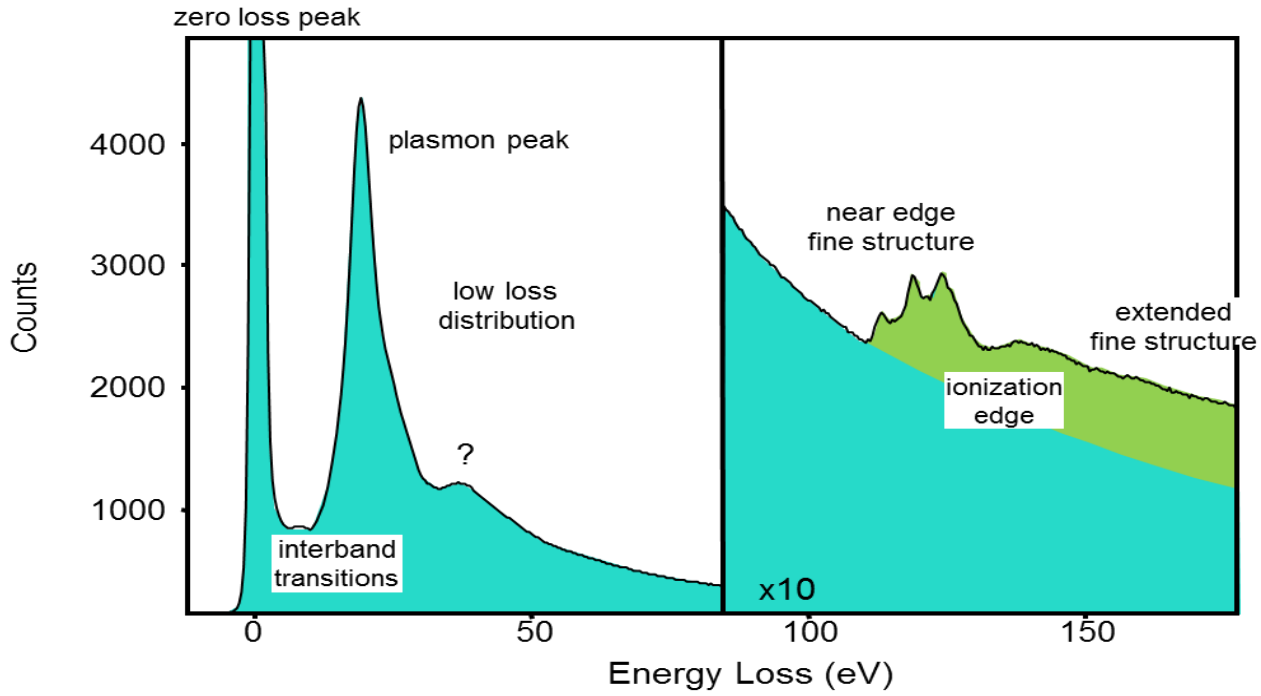


*Figure 14 A typical energy loss spectrum with prominent features with three distinct regions [7].*

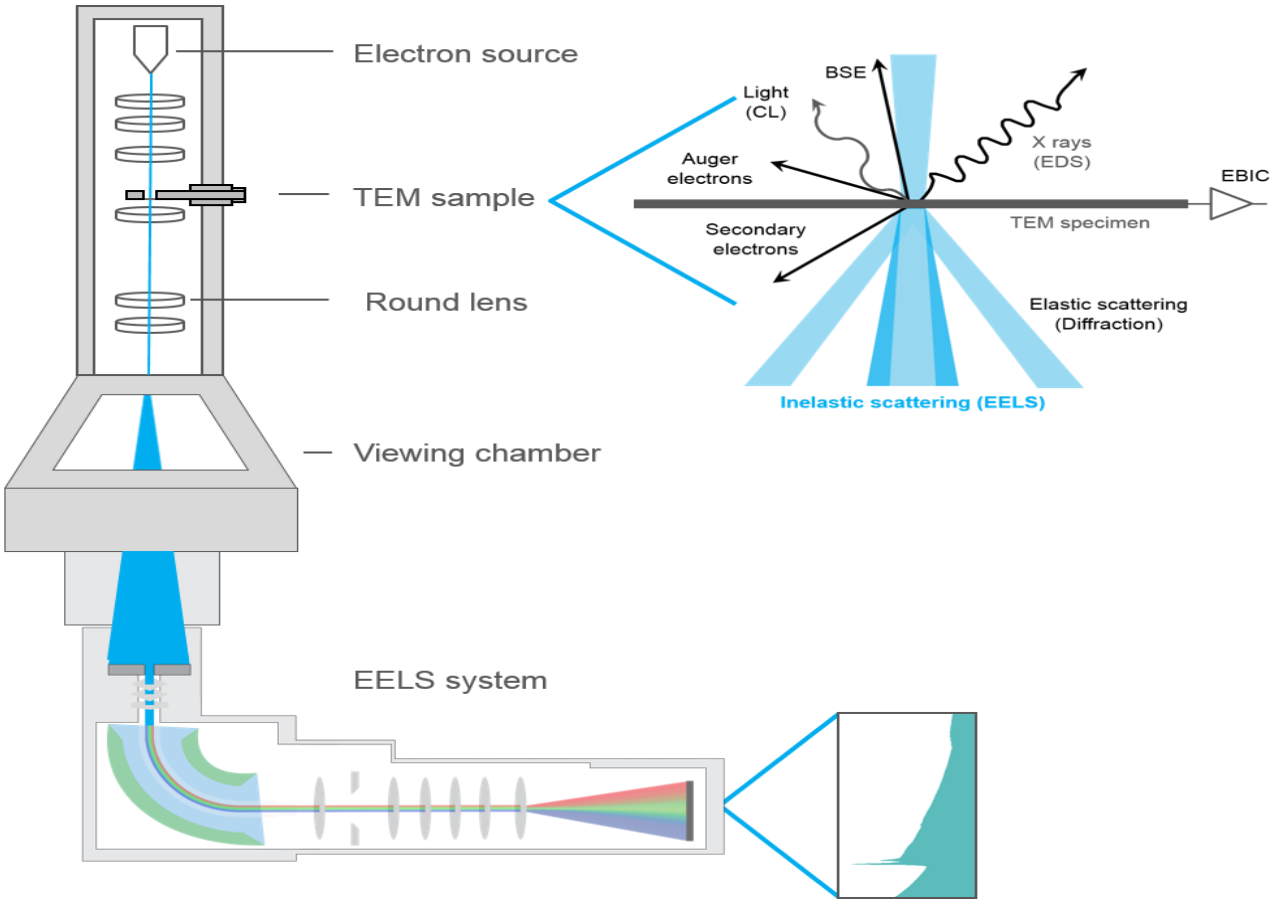


*Figure 15 Schematic view of Acquisition of spectrum image with EELS spectrum [7].*

## 2.4 Acquisition of Spectrum Image/Data Cube

From figure 15 we can see the primary view of generating SI using STEM and from equation (8) electron probe scans the specimen line by line in raster format and generates the three dimensional SI or data cube. The electron beam after passing through the sample finally enters into the spectrometer(fig. 16) which is a magnetic prism which disperses the electron trajectories along one direction as a function of energy and at the edge a scintillator is attached to the imaging plane. The electron generated photons are transferred onto a 2D camera either through optical fiber system or by lens coupling and the camera is a rectangular CCD(charged coupled device) 1000*100 pixels whose read out must be synchronized with the probe movements during the acquisition of spectrum image [5].

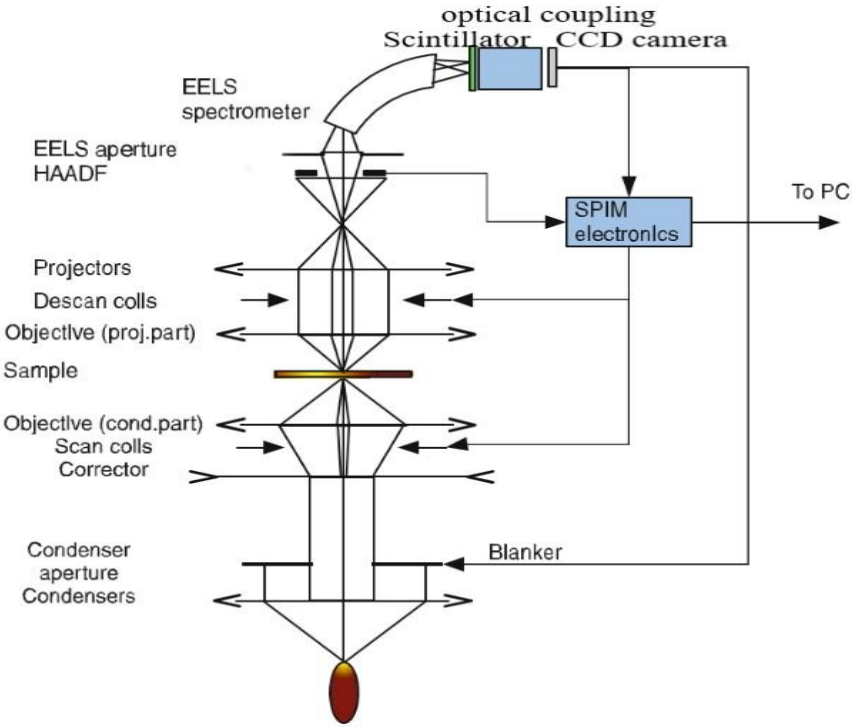


***Figure 16 Acquisition of Data cube in STEM mode for $C_s$ corrected probe system [5].***

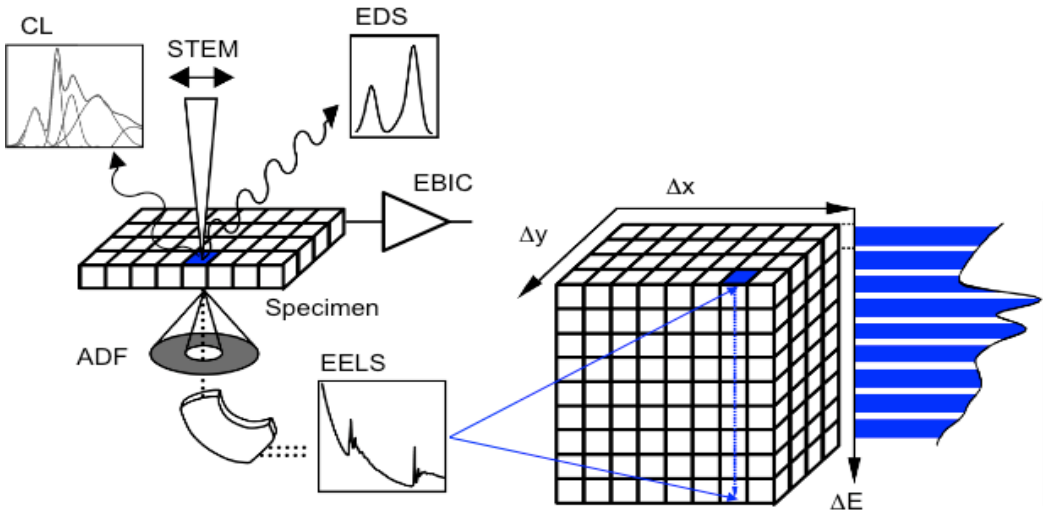


***Figure 17 Generation of EELS data cube in STEM mode [7].***

## 2.5 Data Cube

A data cube is a 3d or higher range of values predicting the time sequence of an image's data. Data cube shown in figure.18 of (a) is a 3d or higher range of values that are generally used to explain the time sequence of an image 's data to evaluate aggregated data from different viewpoints which is mandatory in imaging spectroscopy as (x, y) in fig.18 (c) depict the position of specimen in 2D probe position and along Z - direction I(ΔE) represents beam of voltage with energy loss in fig. (b) [3].

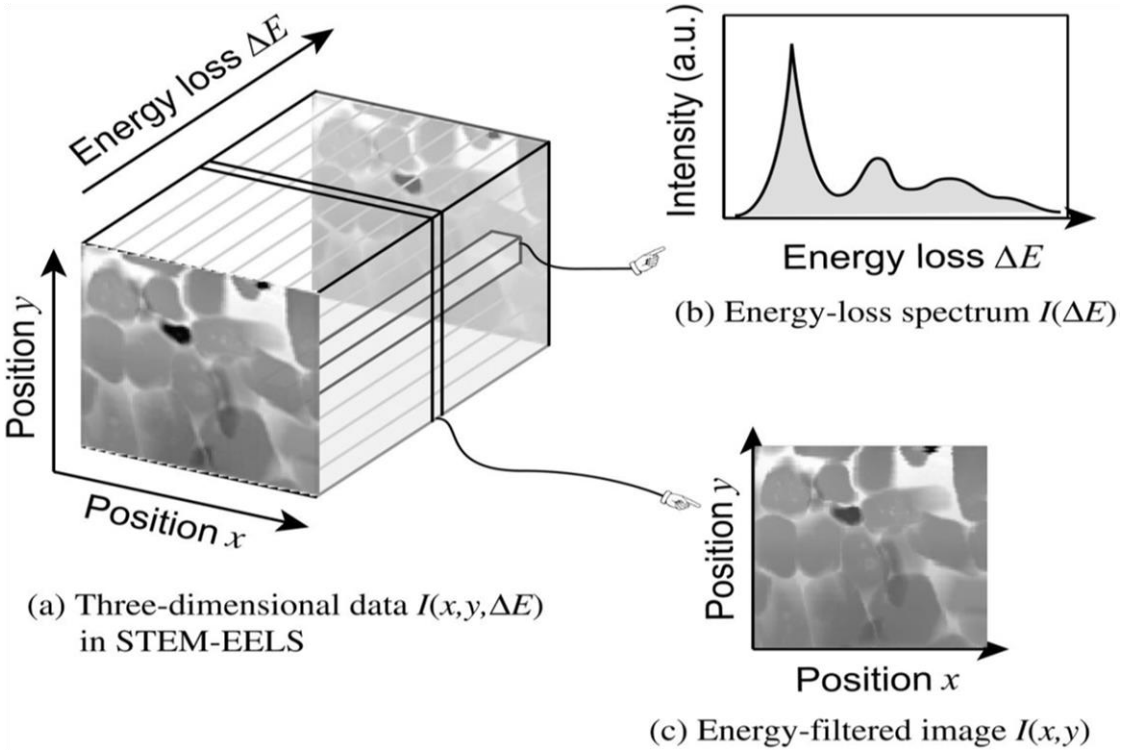


***Figure 18 Schematic view of 3D data cube in STEM SI:* (a) *3D data cube I(x, y, ΔE),* (b) *EEL spectrum and* (c) *Energy -filtered image constructed from the 3d data cube [3].***

# 3 Data Analysis

The obtained data cube consists of 100*100 pixels with a range of CCD 2048 bins which demands statistical methods to extract bulk information of specimen. Analysis of SI method offers post acquisition treatment of elemental maps including conventional spectral processing techniques such as background correction and signal deconvolution and hence by doing this method minor elements presence could be extracted for mapping but characterizing elemental fluctuations in nanometer and angstrom scale could not be that much easy because STEM suffers weak signal due to low amount of specimen volume and high voltage vs sample damage vs time of acquisition for each pixel with accordance to each energy channel. Weak signals in elemental mapping can be enhanced by using advanced statistical techniques which combine the numerical algorithms. The multi variance statistical method(MSA) is one of the best method to investigate EELS data cubes in an unsupervised way. These tools can greatly reduce the noise present in EELS data sets and can give the clear cut information about material spectrum or elemental information through SI method for a user. The reduced noise free data can be reconstructed by removing random noise data sets and the reconstructed data or SI can be used for fingerprint of materials. Dealing with such huge spectroscopy data sets can be done by using **'Gatan Digital micrograph suite DMS'** software with integration of MSA plugin. Principal component analysis is one of the indispensable tool of MSA plugin methods developed to deal with SI.

## 3.1 Principal Component Analysis

The principal component analysis is used theoretically to extract spectrum and elemental maps by filtering noise present in SI or data cube. So, let us understand the statistical theory behind PCA step by step with examples [8]:

Statement : A statistical mathematical algebra technique that examines the interrelations among any data sets(EELS,EDX) of variables and identify the underlying structure of those variables from 'n'-dimensional to 2-dimensional by using diagonalization of the covariance matrix where eigen vectors represent spectra as a function of their associated eigen values and first few eigen vectors contains highest variance used for reconstruction by neglecting the eigen vectors with least variance contributing noise. The assumptions of PCA are [9] :

1. 'Linearity'-Assumes the data set to be linear combination of the variables
2. 'Mean &Covariance'-Not sure whether the directions of maximum variance exists with good features for discrimination.
3. 'Large variances have important dynamics'-Larger variance components exhibits greater dynamics while lower ones corresponds to noise.

Theory : Data cube or data matrix consists of several pixels as many as 100*100 pixels each pixel in hyperspectral image or SI contains spatial positions of x, y directions with STEM probe intensity in Z direction which gives spectrum in each pixel. As a result, there is high data to find interrelation between the variables. PCA technique can clearly suit for this data analysis and can significantly improve the signal to noise ratio. The mathematical expression for PCA is

$$A_{((x,y),E)} = UV^T \dots\dots\dots\dots\dots\dots (15)$$

Where A is an original data set, U is m*n score matrix and V is an n*n loading matrix. Matrices T and V can be found instance from the Singular value decomposition algorithm of A: [10]

$$\boldsymbol{A = U\,\Sigma V^T} \dots\dots\dots\dots (16)$$

In EELS, we unwrap two spatial dimensions to obtain data matrix A with dimensions $p \times N_E$ where p is the total amount of spatial positions and $N_E$ is the amount of pixels in each spectrum and $T=U\Sigma$, $\Sigma$ is the diagonal matrix which gives the total variance of 'A' which is known as 'principal component' and is most important for avoiding the noise in data set. U &Vis formed with the cross product of $A*A^T$ and $A^T*A$. Let's understand this whole SVD algorithm step by step with an example of 3d matrix.

Let A be 3*3 matrix with rank3, $A = \begin{bmatrix} 1 & 5 & 3 \\ 2 & 7 & 9 \\ 4 & 8 & 6 \end{bmatrix}_{3*3}$

Now apply equation 16 where we can decompose matrix into three different forms and extract highest variance.

**Step-1:** $U = \frac{1}{\sigma} A * v_i \Longrightarrow A * A^T = \begin{bmatrix} 35 & 64 & 62 \\ 64 & 134 & 118 \\ 62 & 118 & 116 \end{bmatrix}$

**Step-2:** calculate eigen vectors for $A*A^T$ with $|A * A^T - \lambda I| = 0 \dots\dots (17)$ where I is identity matrix.

$$\begin{bmatrix} (35-\lambda) & 64 & 62 \\ 64 & (134-\lambda) & 118 \\ 62 & 118 & (116-\lambda) \end{bmatrix} = 0$$

Therefore, we will get an equation from step 2 as ***( $\lambda^3$-285$\lambda^2$+2430$\lambda$-2916=0)---(18)*** and this equation requires 'Newton Raphson method' where we get iterations and repeated value as outcome. The eigen values of matrix A are;

***$\lambda$ = 1.44297, 7.31547, 276.24156*** now compute this values in eq.17 to get eigen vectors(v) for each eigen value($\lambda$) in descending order and we get,

For $\lambda 1=276.24156 \Longrightarrow v_1 = \begin{bmatrix} 0.54175 \\ 1.07333 \\ 1 \end{bmatrix}; \lambda 2 = 7.31547 \Rightarrow v_2 = \begin{bmatrix} 0.51366 \\ -1.19094 \\ 1 \end{bmatrix}$ and

$$\lambda 3 = 1.44297 \Rightarrow v_3 = \begin{bmatrix} -1.89238 \\ 0.02348 \\ 1 \end{bmatrix}$$

calculate the length of each eigen vector using $L = \sqrt{(\Sigma x_n^2)}$ and normalize them by means of individual vector with

$$u_1 = \left(\frac{0.54175}{1.56382}, \frac{1.07333}{1.56382}, \frac{1}{1.56382}\right) = (0.34643, 0.68635, 0.63946)$$

and similarly, $u_2$ and $u_3$ which gives,

$$U = \begin{bmatrix} 0.34643 & 0.68635 & 0.63946 \\ 0.68635 & 0.72718 & 0.01098 \\ 0.66503 & 0.71733 & 0.20775 \end{bmatrix}_{3*3}$$

and alternatively, V is calculated in same method that has applied for calculating U.

$$V = \begin{bmatrix} 0.25733 & 0.48126 & 0.83795 \\ 0.70108 & 0.50381 & -0.50466 \\ 0.66503 & -0.71734 & 0.20774 \end{bmatrix}_{3*3}$$

and now we calculate 'Σ' the diagonal matrix or correlation matrix which gives the variance of A. 'Σ' can be calculated from U&V eigen values in descending order with their mean squared roots which, gives the same result compared from U and V:

$$\Sigma = \begin{bmatrix} \sqrt{\lambda_{pc1}} & 0 & 0 \\ 0 & \sqrt{\lambda_{pc2}} & 0 \\ 0 & 0 & \sqrt{\lambda_{pc3}} \end{bmatrix} where\ eigen\ values of \left(\sqrt{\lambda_{pc1}} > \sqrt{\lambda_{pc2}} > \sqrt{\lambda_{pc3}}\right) \ldots (19)$$

and each one of the vector in diagonal matrix is single principal component. From U, eigen values are computed in Σ

$$\Sigma = \begin{bmatrix} \sqrt{276.24156} & 0 & 0 \\ 0 & \sqrt{7.31547} & 0 \\ 0 & 0 & \sqrt{1.44297} \end{bmatrix} \Rightarrow \begin{bmatrix} 16.62052 & 0 & 0 \\ 0 & 2.70471 & 0 \\ 0 & 0 & 1.20124 \end{bmatrix}$$

From 'Σ' we have first two vectors in diagonal matrix correspond to most of the variance in the matrix A. Hence, we can neglect the remaining principal components and avoid noise which is the notion implemented in spectrum extraction. PC's 1&2 have the 95% of dynamics which can explain A. By using PC1 and PC2 we can reduce the 3dimensional data to 2d dimensionality maintaining all the dynamics of initial data. So, lets reconstruct by using PC1 and PC2.

**Step-3:** Reconstruction

$$U\Sigma V^T = \begin{bmatrix} 0.3464 & 0.3136 \\ 0.6864 & -0.7272 \end{bmatrix} * \begin{bmatrix} 16.62052 & 0 \\ 0 & 2.70471 \end{bmatrix} * \begin{bmatrix} 0.2573 & 0.7011 \\ 0.4813 & 0.5038 \end{bmatrix}$$

Therefore, we got $\begin{bmatrix} 1 & 5 \\ 2 & 7 \end{bmatrix}_{2*2}$ as reconstructed which is equal to two dimensional matrix of A. If we want the full original A add all the PC's and vectors of U&V. Hence, the above explained theory is applied for SI for filtering noise and getting clear spectrum. Extracting number of principal components depends upon the dimensionality of data sets. To check how much percentage of A data is accounted in principal components or estimate how much of A is accountable in principal component sets we use;

$$Trace\ of\ (A)\% = \left(\Sigma \frac{Selected\ sum\ of\ PC's}{Total\ sum\ of\ all\ PC's}\right) \times 100 \ldots\ldots (20)$$

From the obtained PC's of matrix, A, we apply eq.20 and check how first two PC's are consisting data% of A:

$Trace\ of\ A\% = \frac{16.62052+2.70471}{16.62052+2.7047+1.20124} \times 100 \Rightarrow 94.14\% \cong 95\%$ of data from A, by reducing 3d to 2d and these applies for multidimensional data sets too where the final consideration of highest variance of dynamics is found in first few principal components and the rest would be noise of the SI.

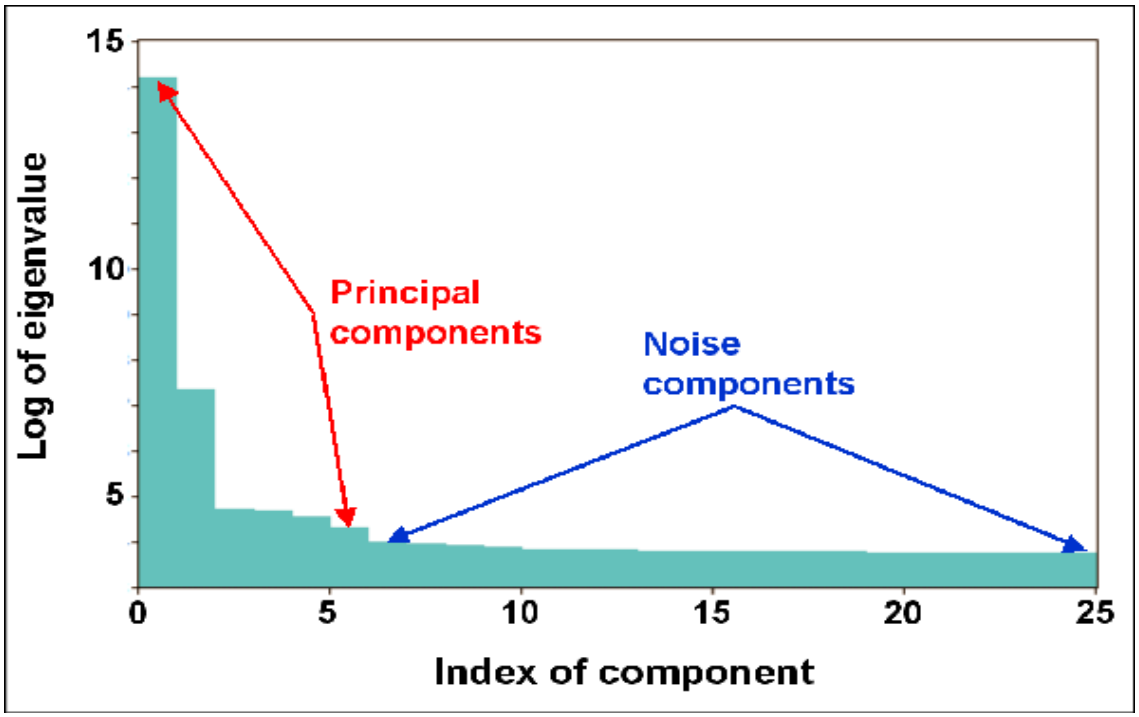


***Figure 19 An example of the scree plot generated after PCA decomposition in the PCA plugin** [11].*

## 3.2 Quantification of EELS

EELS quantitative elemental analysis requires extraction of the characteristic inner shell signals and determination of the appropriate ionization cross sections. Accuracy of determining elemental compositions depends on certain techniques for background estimation and signal extraction, and the methods of linear least squares fitting of reference spectra and in case of thick specimens the spectra is distorted by plural inelastic scattering which can be removed by deconvoluting the spectral intensity to yield single scattering distributions. Detection limits can be estimated from the signal/noise and particular element is analyzed. With the spectrum imaging method, it is now feasible to measure atomic concentrations < 100 ppm in a single pixel of an elemental map and to detect single atoms of certain elements. EELS is developed highly sensitivity in detecting very small number of atoms which makes the user having advantage over EDX for analyzing the light elements that have a low fluorescence yield and also EELS is also preferable to EDX for analyzing certain heavier elements [12]. To quantify EELS, we depend on two main factors,

a) Separating the characteristic core edge intensities from the non-characteristic background(background in the spectrum, noise, artifacts, etc..).
b) Determination of the elemental composition requires information about the low loss spectrum and the information of the acquisition parameters such as collection geometry(finite convergence angle α, displacement of the collection aperture β, sample orientation τ), beam energy, detector response and also the inner shell ionization cross sections(e.g., hydrogenic, Hartree-Slater) [13].

In addition, we must also consider some factors which can influence the EELS such as thickness of specimen and electron optics of the microscope in a suitable way. The best way to understand quantification is by formulation. The characteristic inner shell signal $S_x$ used for micro analysis is given by,

$$S_x(\Delta,\beta) = J_o n_x \sigma_x(\Delta,\beta)\eta \ldots\ldots\ldots (21)$$

Where, $\sigma_x(\Delta,\beta)$ is the cross section per atom for ionizing an inner shell electron x and η is the detective quantum efficiency of the detector. The partial cross section $\sigma_x(\Delta,\beta)$ is a measure of the ionization probability, whereby the fast electron loses energy from the threshold energy $E_x$ to $E_x + \Delta$ and with scattering angles less than β. The low loss spectrum including ZLP(zero loss peak) is measured from the specimen,

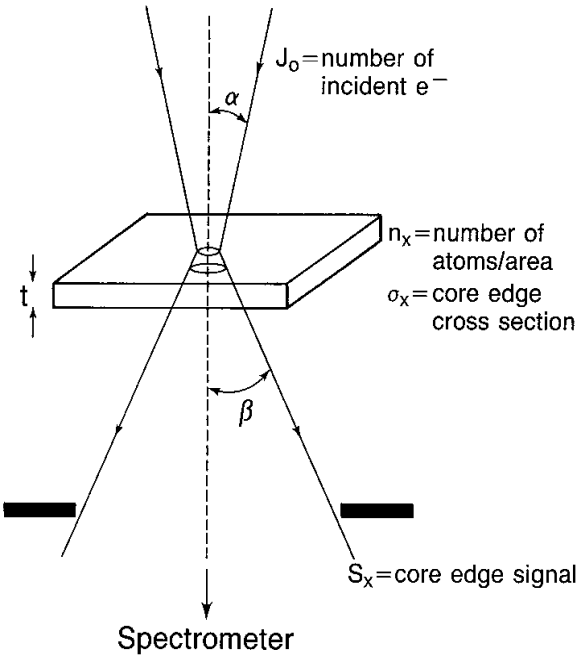


***Figure 20 Scattering geometry in STEM mode and parameters** [12].*

$$S_x(\Delta,\beta) = J_1(\Delta,\beta)\eta_x\sigma_x(\Delta,\beta)\ldots\ldots (22)$$

From eq.22 subscript 1 denotes the LL and ZLP and η(quantum efficiency factor) is neglected. Eq. 22 enables us to determine the total number of atoms per unit area of the sample. If the specified area of the specimen is M, then the absolute number of atoms of element x contained in that region is given by [12],

$$N_x = \frac{S_X(\Delta,\beta)\, M}{J_1(\Delta,\beta)\sigma_x(\Delta,\beta)} \ldots\ldots\ldots (23)$$

The measured low loss and core loss intensities (x & y) are indicated schematically in fig.21 for energy window Δ, integrated core loss signals are obtained by extrapolating the pre edge background fit over energy window Γ by means of an inverse power law [12].

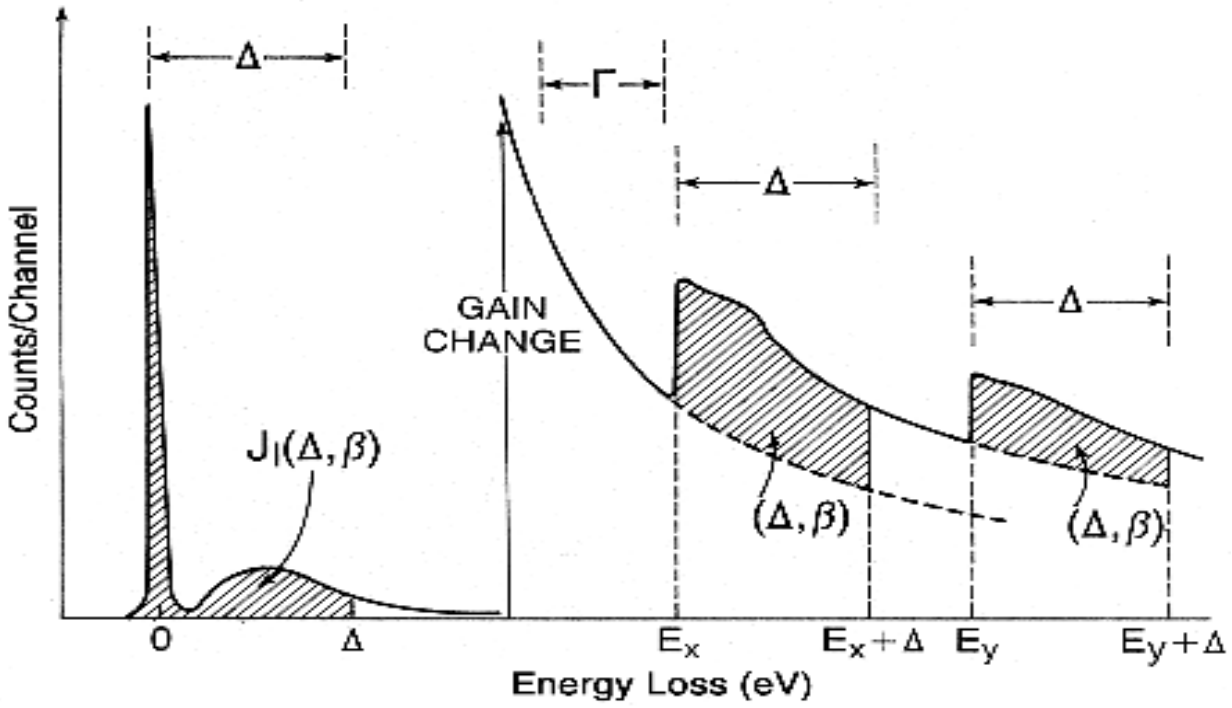


***Figure 21 A example Sample model for defining measured intensities in energy loss spectrum required for quantification using eq.21-24. Shaded regions areas correspond to numbers of counts in integration window Δ. Core edge signals are obtained by extrapolating background modeled using inverse power law over fitting window Γ*** *[12].*

In most microanalytical problems we are more interested in relative numbers of atoms x and y rather than their absolute numbers. The atomic ratio is given simply,

$$\frac{N_x}{N_y} = \frac{S_x(\Delta,\beta)}{S_y(\Delta,\beta)} \frac{\sigma_y(\Delta,\beta)}{\sigma_x(\Delta,\beta)} \quad \ldots\ldots\ldots\ldots (24)$$

## 3.3 Background correction and Signal extraction

For the accuracy and precision we depend on different methods such as simple least-squares fitting for the core edges, that are to be quantified are mostly superimposed on a large background that can be produced by several processes as shown in figure.22 with different contributions (1) background due to detector noise and spurious electron scattering in spectrometer, (2) single scattering tails of valence or lower energy core excitations, (3) plural inelastic scattering involving high energy tails of valence or lower energy core excitations combined with one or more 'plasmon' excitations, (4) single scattering core edge intensity, (5) plural inelastic scattering

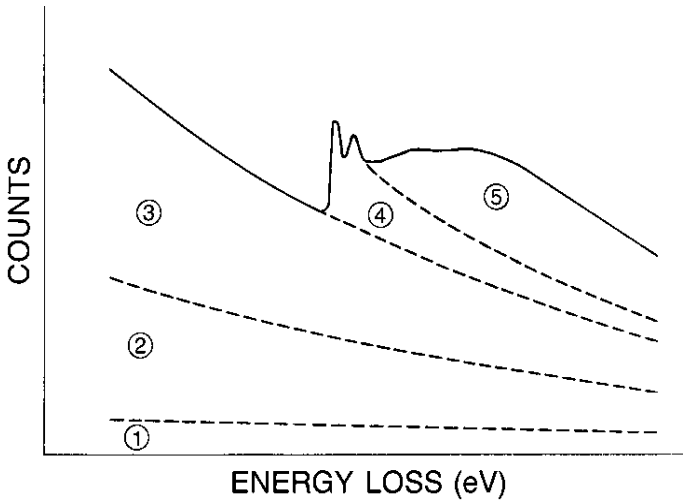


***Figure 22 Different contributions to the core edge spectrum*** *[12].*

involving core excitation combined with one or more 'plasmon' excitations. Despite of all this complications mentioned in fig.22 we use 'inverse power law' for background modelling [12].

$$B_j = AE_j^{-r} \ldots\ldots\ldots\ldots\ldots\ldots (25)$$

Here A and r are constants and j denotes the channel number with corresponding energy loss $E_j$. By applying logarithm to eq.(25) we can fit the background with a straight line and estimate it into the region of the core edge. We use simple linear regression algebraic model and minimize the value of [12]

$$\chi^2 = \sum \left[\frac{ln\, B_j - lnA + r\, ln\, E_j}{\sigma_j}\right]^2 \ldots . (26)$$

Where $\sigma_j$ are the weights associated with channel j. Let us assume $x_j$ = ln $E_j$ and $y_j$ = ln $B_j$ and weights are constant in the fitting region then the constants r & A are given by,

$$r = \frac{\sum x_j \sum y_j - m\sum x_j y_j}{m\sum x_j^2 - (\sum x_j)^2} \ldots\ldots\ldots (27)$$

$$ln\, A = \sum \frac{y_j}{m} + r \sum \frac{x_j}{m} \ldots\ldots\ldots (28)$$

where the sums are computed over all m channels in the fitting region. To minimize the statistical errors in the signal $S_x$ obtained by subtracting the estimated background B, fitting region Γ and the integration region Δ accurately. The variance in $S_x$ is given by the total number of counts in the edge region ($S_x$ + $B$) plus the variance in the estimated value of B: *var* ($S_x$) = $S_x$ + $B$ + *var(B)*. The errors produced by counting statics can be simplified with different statistical measures. The Egerton based expression for signal to noise ratio is,

$$\frac{Signal}{noise} = \frac{S_x}{[Var(S_x)]^{1/2}} = \frac{S_x}{(S_x + hB)^{1/2}} \ldots\ldots\ldots (29)$$

Where h = 1+[var(B)]/B and the pre-edge region should Γ should be as large as possible to minimize the variance in the estimated background [12].

### 3.4 Plural scattering and sample thickness

The EEL spectrum is often complicated by plural inelastic scattering effect which occurs when a significant fraction of incident electrons that pass through a sample are scattered inelastically more than once. As, the sample thickness increases the fraction of electrons in the ZLP falls off exponentially and this behavior is characterized by an inelastic mean free path $\lambda_i$ and EELS can provide at least an approximate value of thickness from both crystalline and amorphous specimens by straight forward integration of the EEL spectrum and $I_z(E)$ is the zero loss intensity then [12],

$$\int I_z(E)\, dE = exp\left(\frac{t}{\lambda_i}\right) \int I(E)\, dE \ldots\ldots\ldots (30)$$

The ratio of specimen thickness t to the characteristic mean free path for inelastic scattering for the material is,

$$\frac{t}{\lambda} = ln\left(\frac{I_t}{I_0}\right) \ldots\ldots\ldots\ldots (31)$$

Where $I_t$ is the total number of electrons in the EEL spectrum and $I_0$ is the number of electrons having lost no energy or simply ZLP.

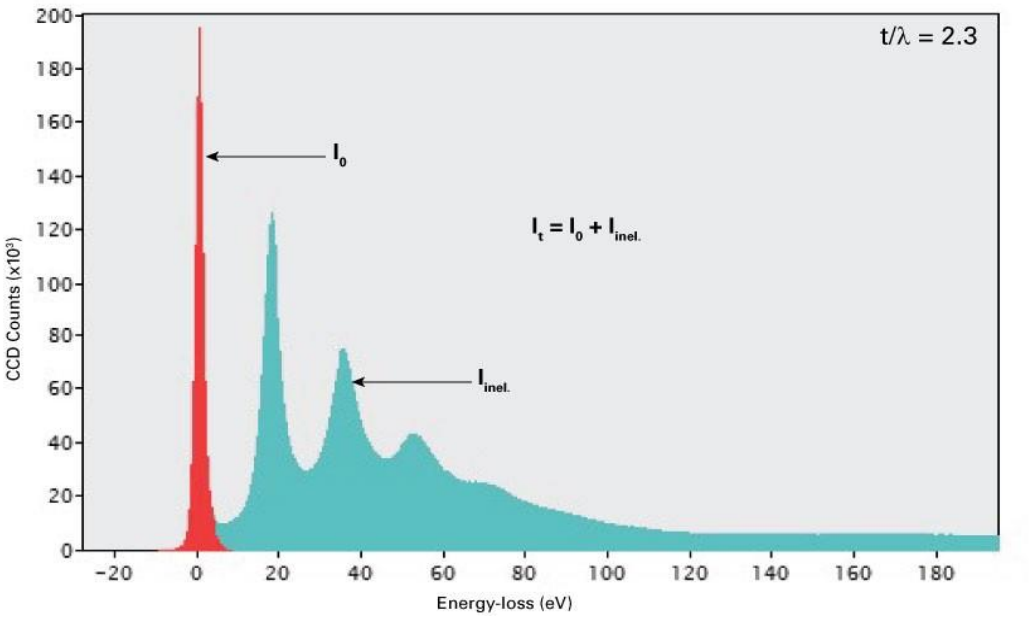


***Figure 23 Typical EEL spectrum showing $I_o$ and $I_t$ from eq.(31) [7].***

## 4 Results

Analysis of EELS and EDX data cubes is investigated with the stated theory of principal component analysis from eq.(16) on dimensionality reduction and feature extraction. For signal extraction and background modelling we depend on power inverse law. Let us examine each material compositions and quantifications. EELS spectrum images are generated in the energy range of 50-2050 eV per 1 eV channel using the background model from eq.(25) and the thickness is calculated from elastic scattering which we consider it as ZLP. The EELS characteristic K-edges or low loss region which has highest valence electrons were modeled by the Hartree-Slater cross sections without considering plural scattering. EDX spectrum images were generated in the energy range of 3-30 KeV with the dispersion of 0.01 KeV using the hyperbolic law for the Bremsstrahlung background and $k_\alpha$, $k_\beta$ lines were modeled by the Gaussian distribution with FWHM. Both EELS & EDX spectrums were scaled with Poisson noise. Throughout the results we filter the SI with PCA and compare from original to reconstructed with accuracy and precision [10].

$$\text{Misfit} = A[(R-O)] \ldots\ldots\ldots\ldots\ldots (32)$$

Where R, O represent original and reconstructed SI and A is the average weighted spectrum of all pixels. In general, we will proceed with PCA model for one sample(al, mg, o) and for other samples we will go straight forward methods for explanation in order to avoid lengthy methods.

***Table.1 Samples used for elemental compositions and quantification, atomic maps [10].***

| Elements | Data Type | Pixel Size/Dimensions |
|---|---|---|
| Al, Mg, O | EELS | 100*100*2000 |
| $SrTiO_3$ | EDS | 66*27*2048 |
| Si-Ge | EDS | 272*220*2048 |

## 4.1 Simulation of EELS data

### a) Al, Mg, O :

The combination of Al, Mg, O compounds SI was taken from the range of 48eV-200eV energy. In the figures 24 white region corresponds to particular element signal distribution and black region corresponds to background signal distribution of that element.

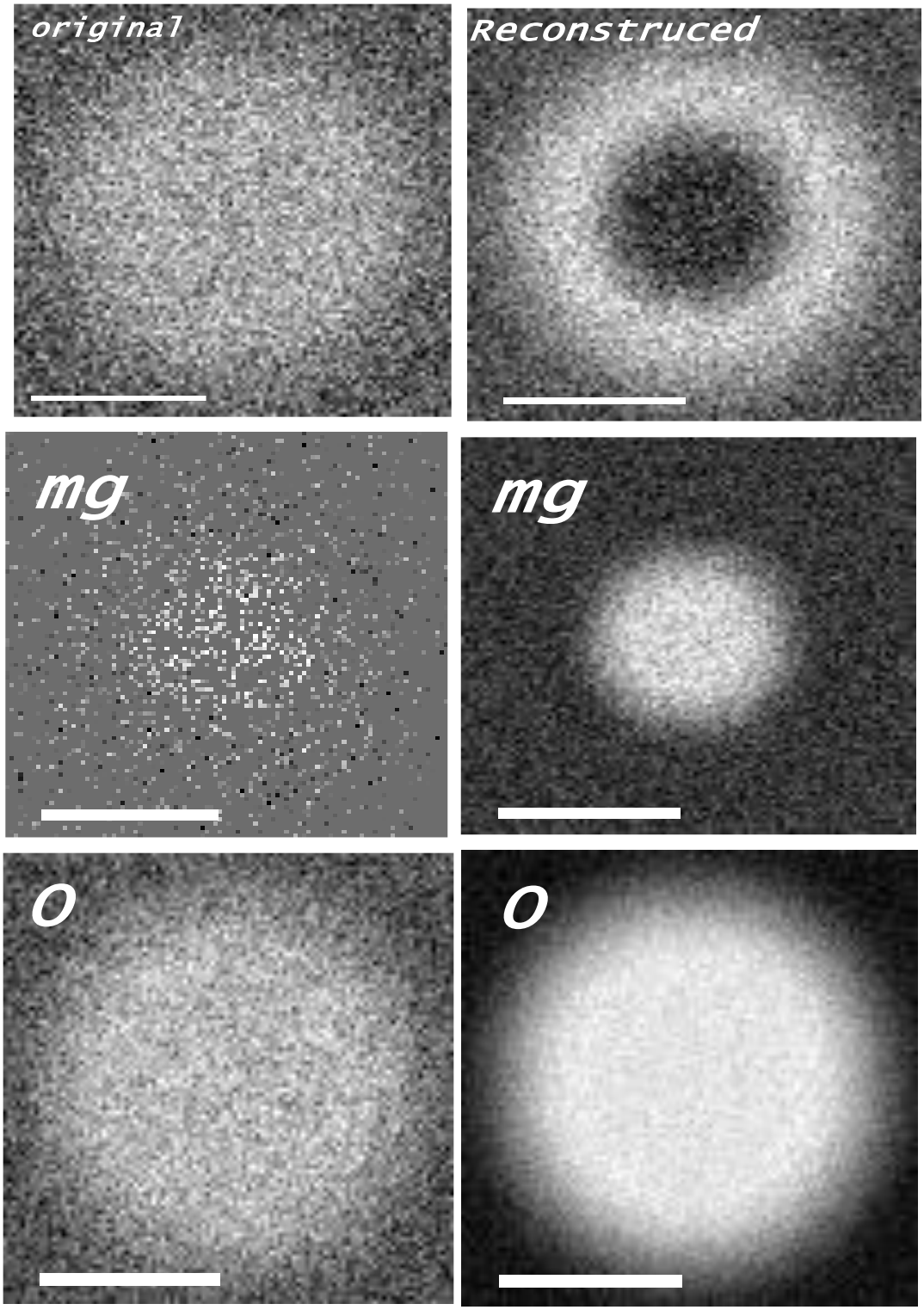

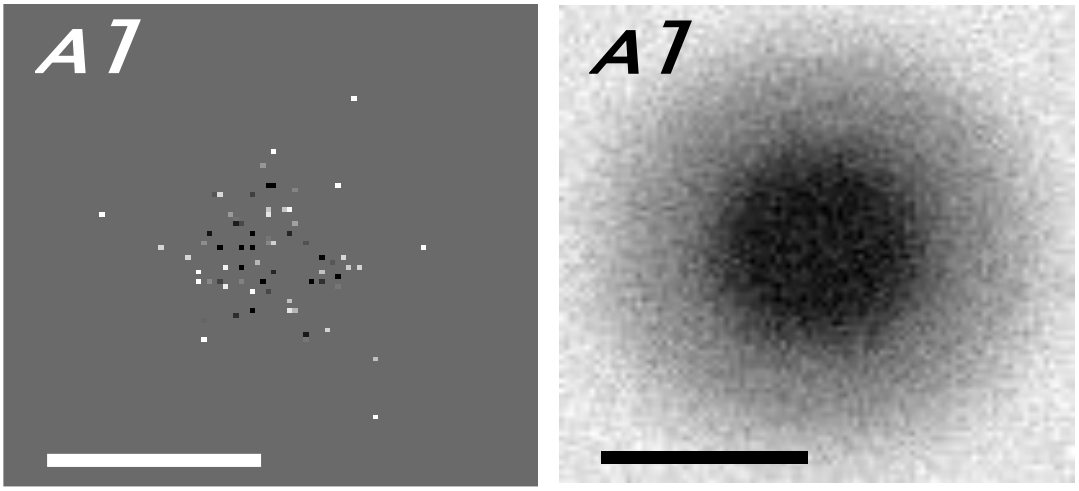


*Figure. 24 Al, Mg, O compounds SI. Original image is a mixture of pure noise and reconstructed shows noise filtered by PCA. Elemental maps extracted of individual elements before and after PCA treatment. Left column images are noise in contrast to right images with PCA filtered noise. Left column shows images pure before PCA and right columns is the improved maps after PCA.*

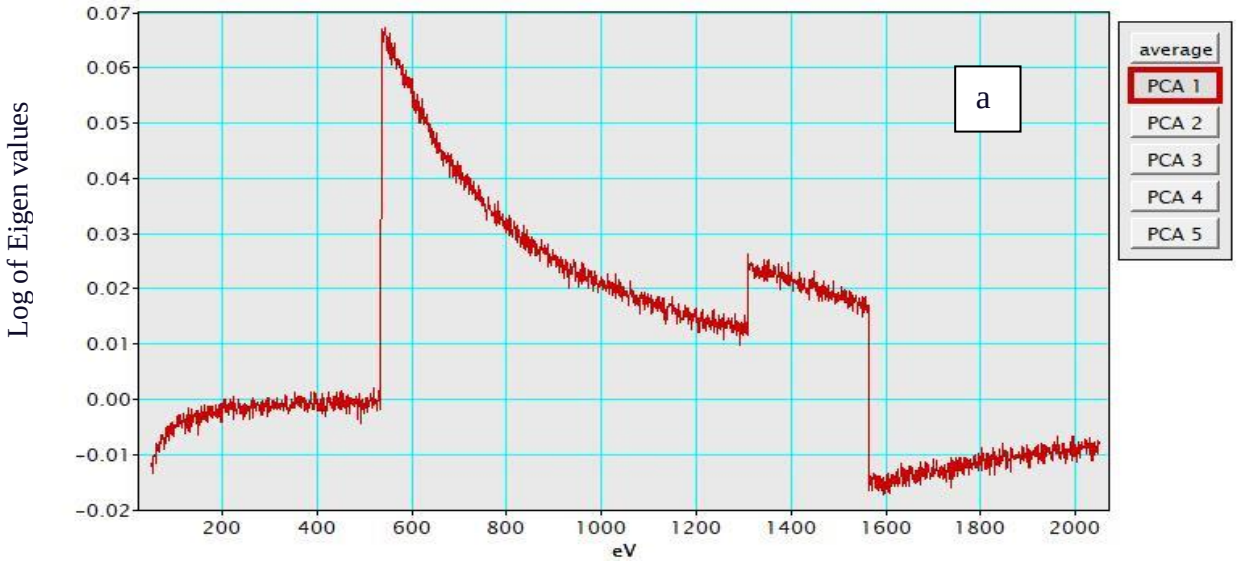


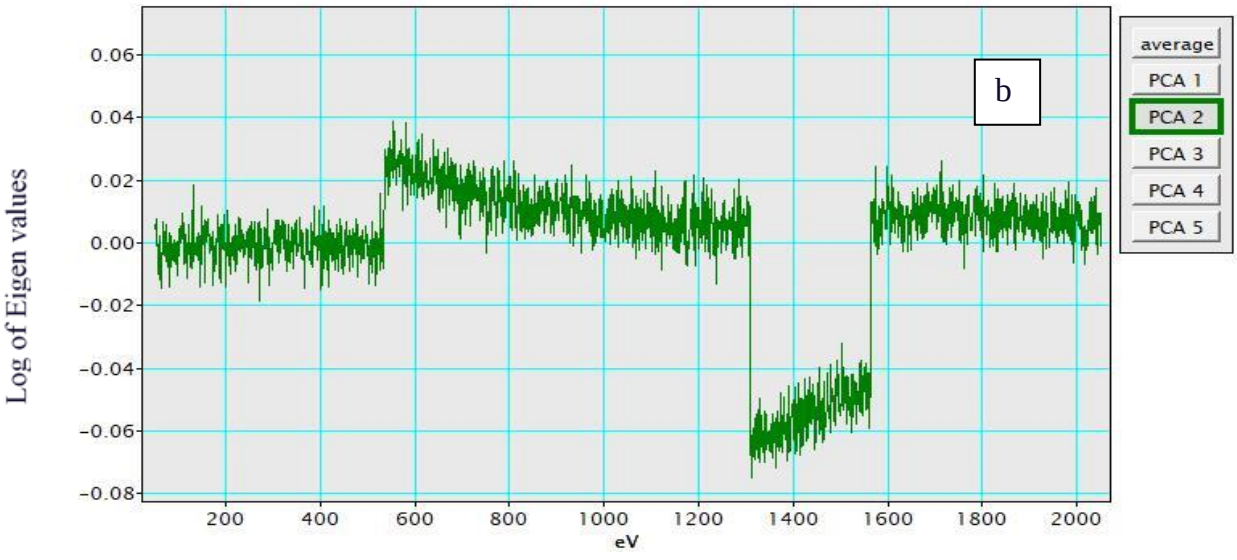

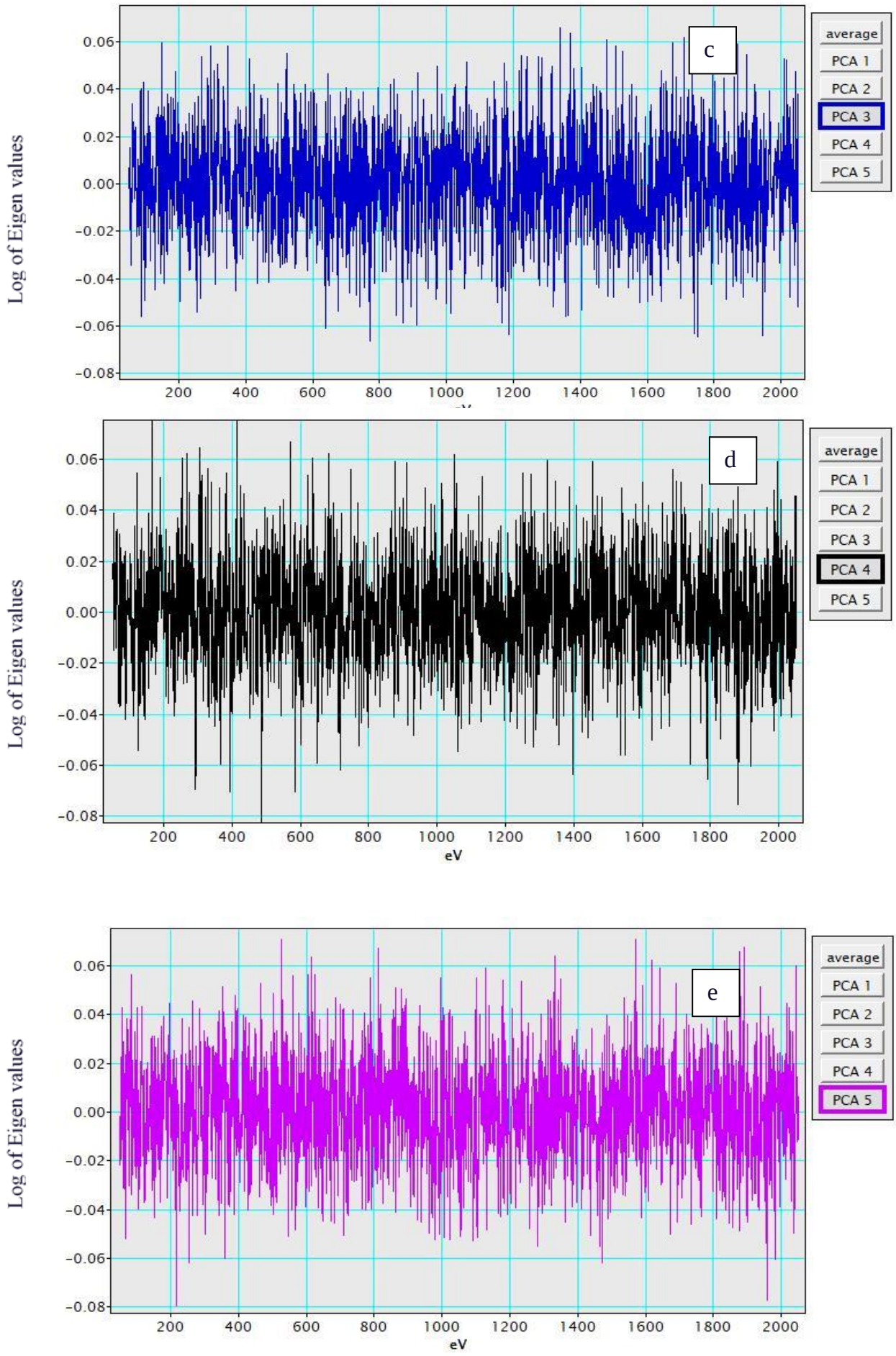


***Figure.25 Unweighted Loadings of PCA 1 to 5 marked as a,b,c,d,e where a, b represents some signal distribution in the spectrum whereas c, d, e shows uneven signal in spectrum which we consider as noise .***

By centering the averaged spectrum, we extracted Principal components and there is no limit of specific number of PC's to obtain as many as PC' s can be extracted, and cross check with PC's having highest variance of dynamics. Accuracy of considering specific number of PC's depends on histogram of components as shown in fig. 19. Only first few components holds the highest data variance. Data variance can be negative or positive if, numbers in the data is in negative values in histogram which doesn't mean the energy is in negative. From figure. 26 we can see first two components are having different variance and the remaining three PC's hold no significant variance to consider. So, for reconstruction in figure 27 we consider only first two PC's and rest will be disregarded.

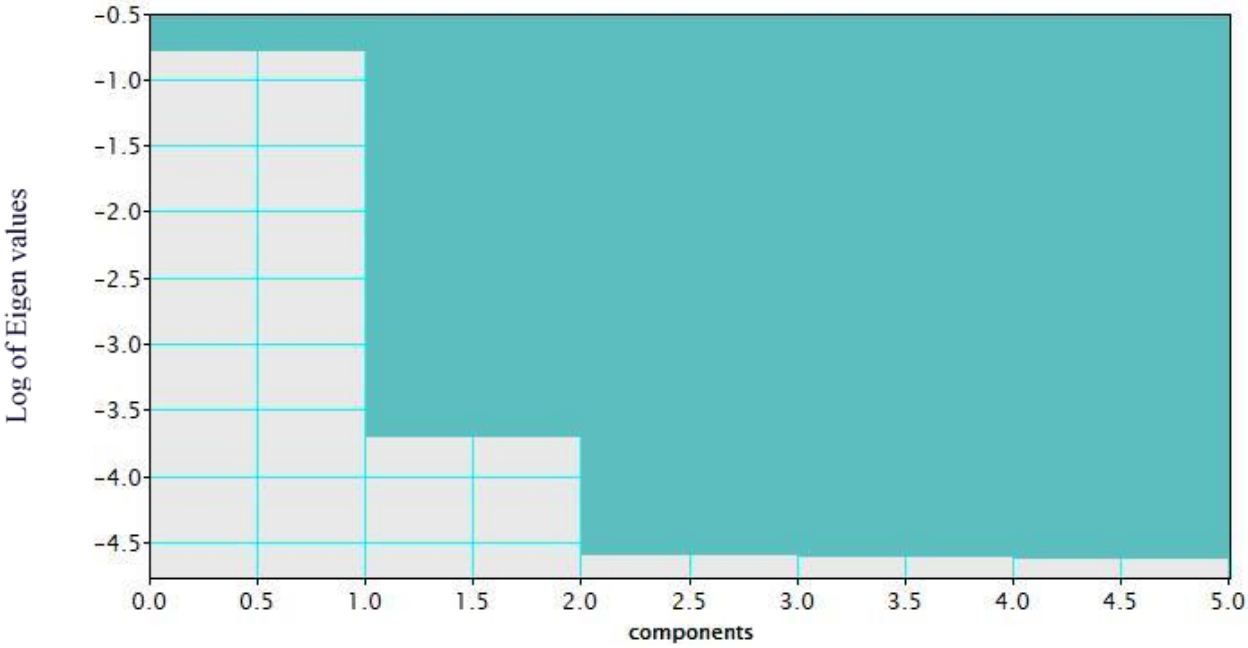


*Figure 26 Histogram Data variance of PCA 1 to 5 only first two PC's showing variance*

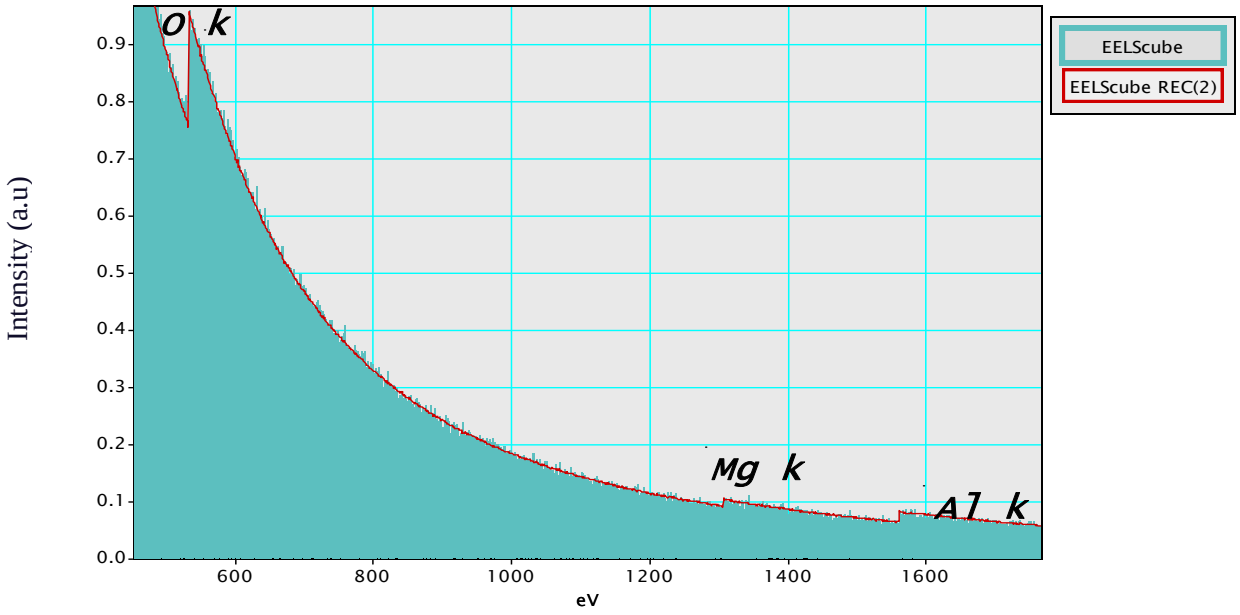


*Figure 27 Shows the original(EELS cube) and reconstructed(EELS cube rec2) and red is the margin for difference of PCA denoised.*

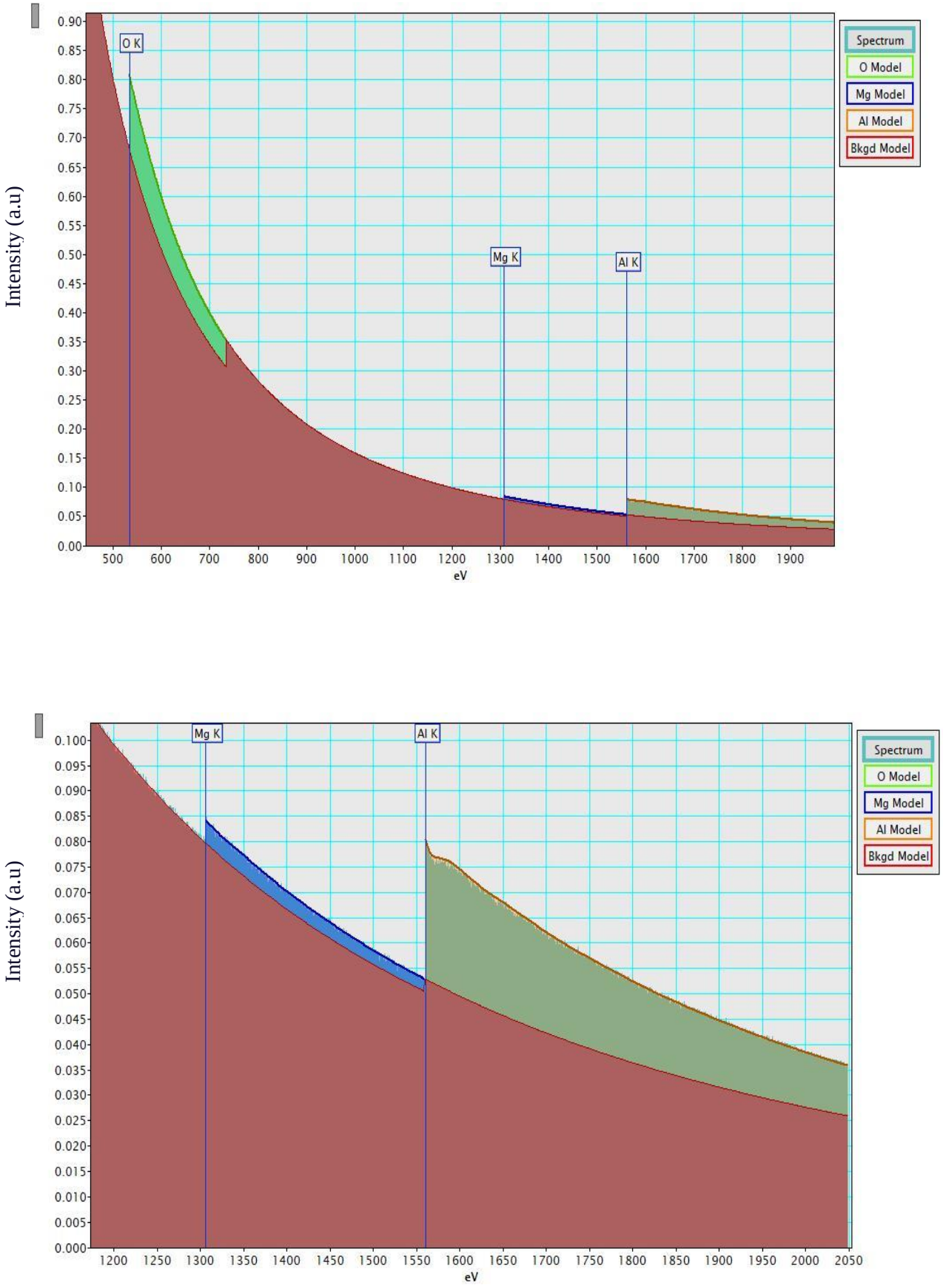


*Figure 28 Power law Background corrected with elemental K-edges of Al, Mg, O*

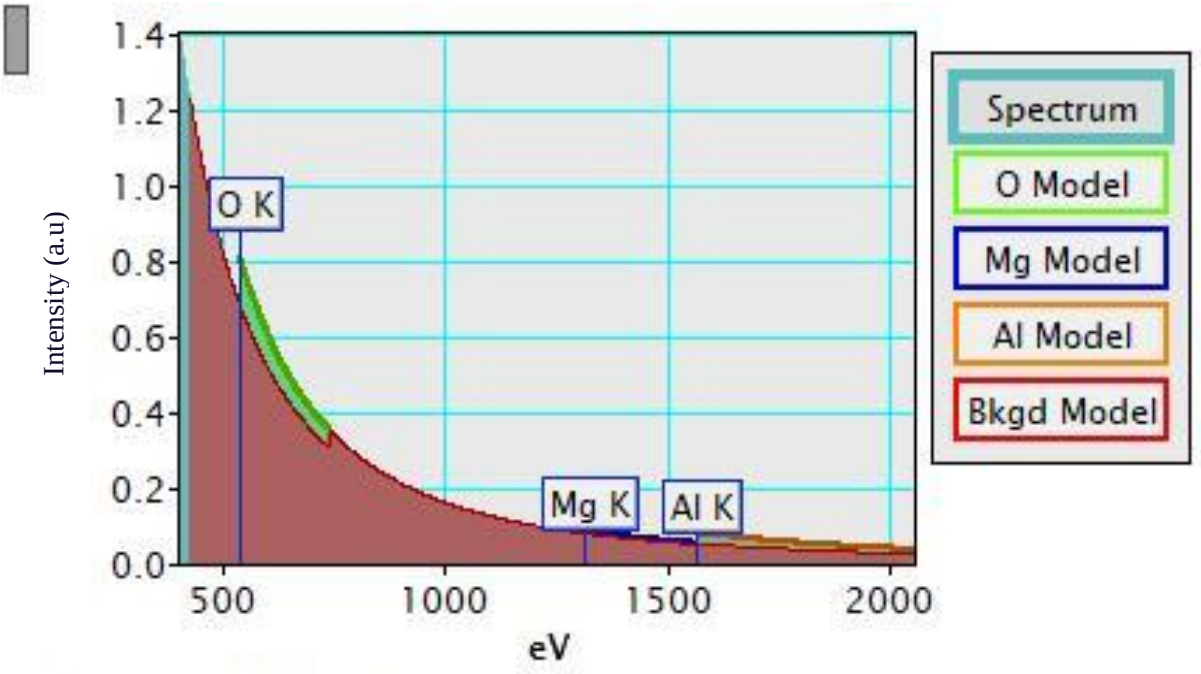


**Experimental Conditions**

Beam energy (keV): 200.0
Collection semi-angle (mrad): 38.9
Convergence semi-angle (mrad): 11.0

**Analysis Information**

Plural scattering not included

**Composition Results**

| Element | Shell | Signal (counts) | Comp. (at.%) | X-section (barns) | X-section Model |
|---|---|---|---|---|---|
| O | K | 11.3 ± 16.6 | 26.4 | 2316.1 ± 115.8 | Hartree-Slater |
| Mg | K | 0.67 ± 15.1 | 7.1 | 509.5 ± 25.5 | Hartree-Slater |
| Al | K | 7.1 ± 28.2 | 66.5 | 578.9 ± 28.9 | Hartree-Slater |

*Figure 29 Analysis report of atomic % of each element*

From fig. 28 we separately showed the background and each element model using eq.(25) and from eq.(24) we calculated the atomic ratio of individual elements composition and the quantification of EELS spectra can be cross checked with EELS chart which has a specific energy range for every element in periodic table. The elemental maps of al, mg, o were obtained after PCA filtered noise and through a standard quantification by inverse power law in the pre edge regions(477-532 eV for O, 1180-1330 eV for Mg, 1565-1600 eV for Al). To calculate thickness, we consider ZLP elastic scattered signal

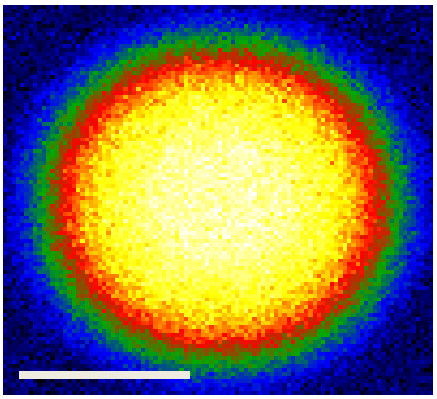

*Figure 30 Thickness map with high contrast*

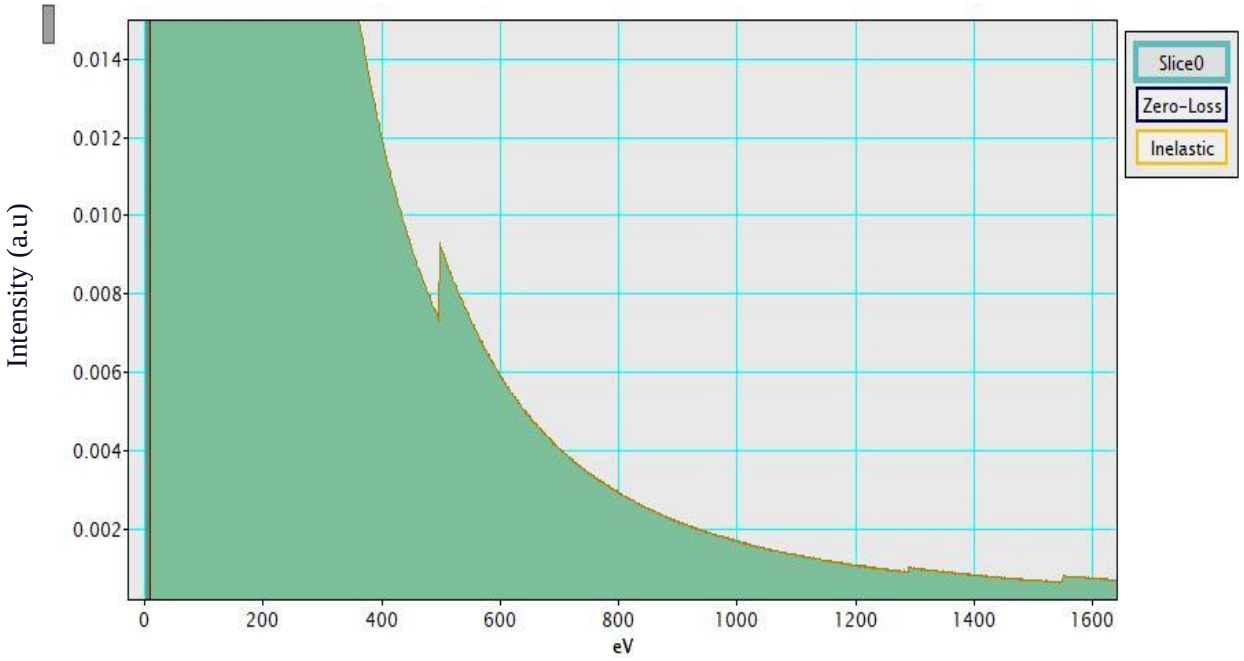


*Figure 31 Calculating Zero loss Peak(0-3 eV) for thickness measurement of specimen.*

## Clustering :

Clustering is a factor of identifying or grouping one group of signal distribution having same characteristics which can be done by looking through the visual inspection of scatterplots of PCA 1 and PCA 2 which has some signal differentiation.

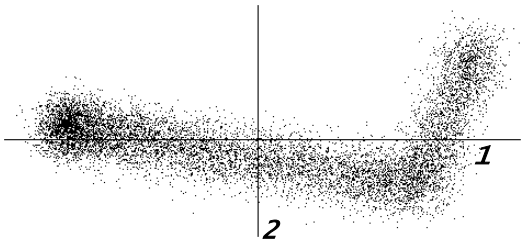


*Figure 32 un clustered scatter plot of pca1 along X-axis and pca 2 along Y-axis.*

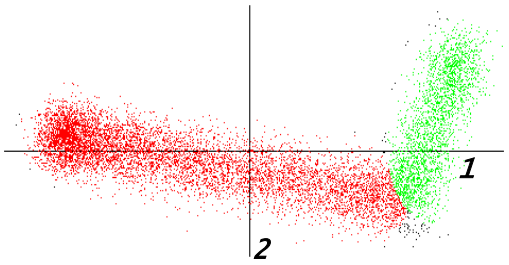


*Figure 33 clustered scatter plot of pca1 along X-axis and pca 2 along Y-axis*

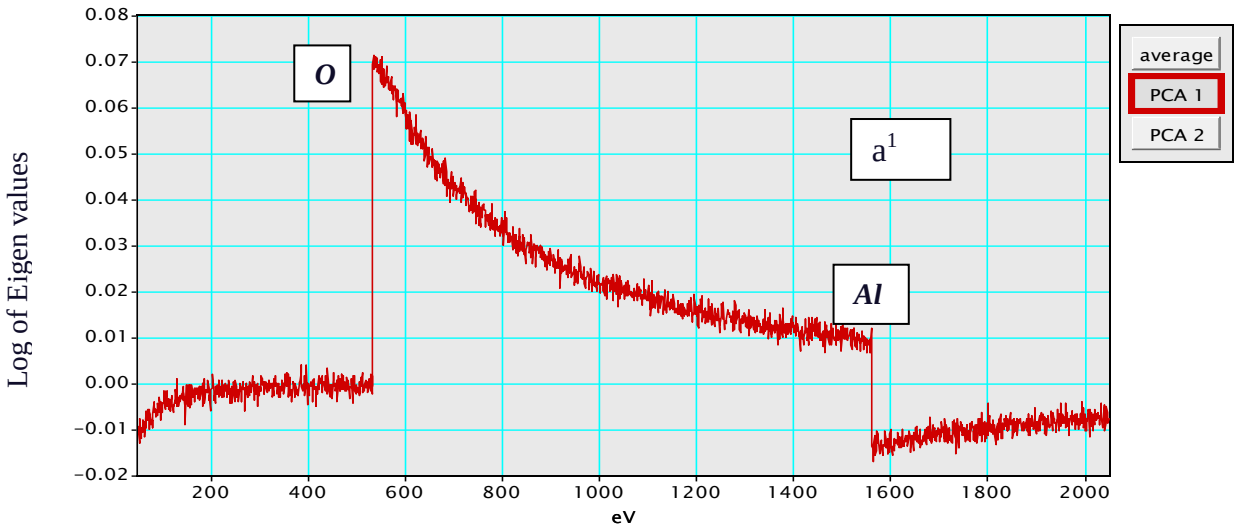

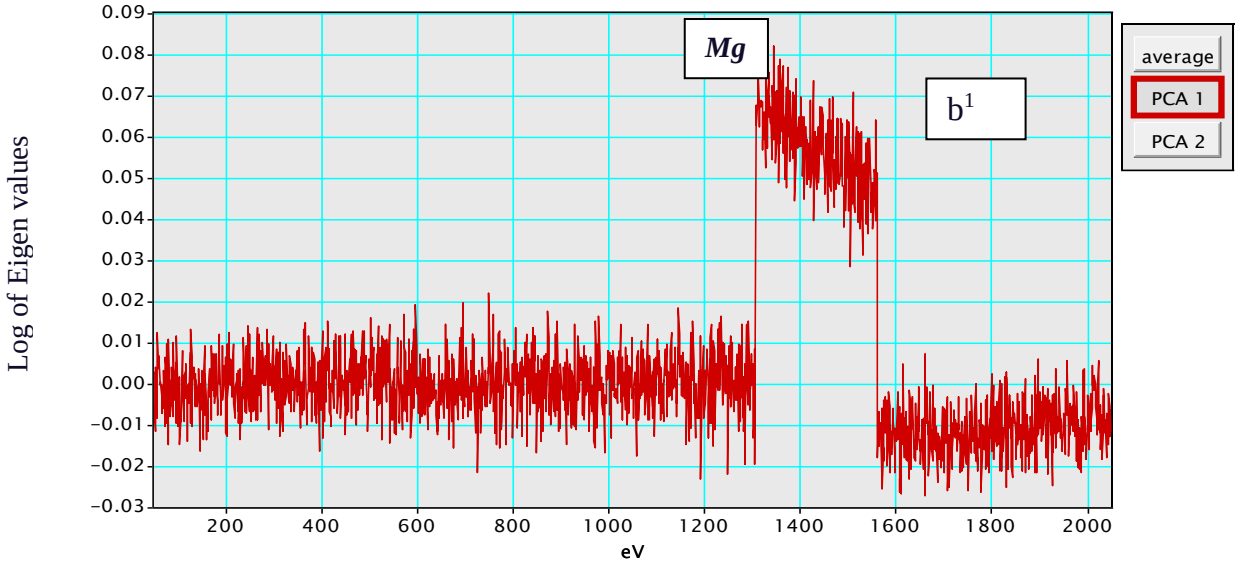


*Figure 34 Clustered PCA1 and PCA2 as $a^1$ and $b^1$ in contrast to figure 25 a and b which means spectrum is averaged.*

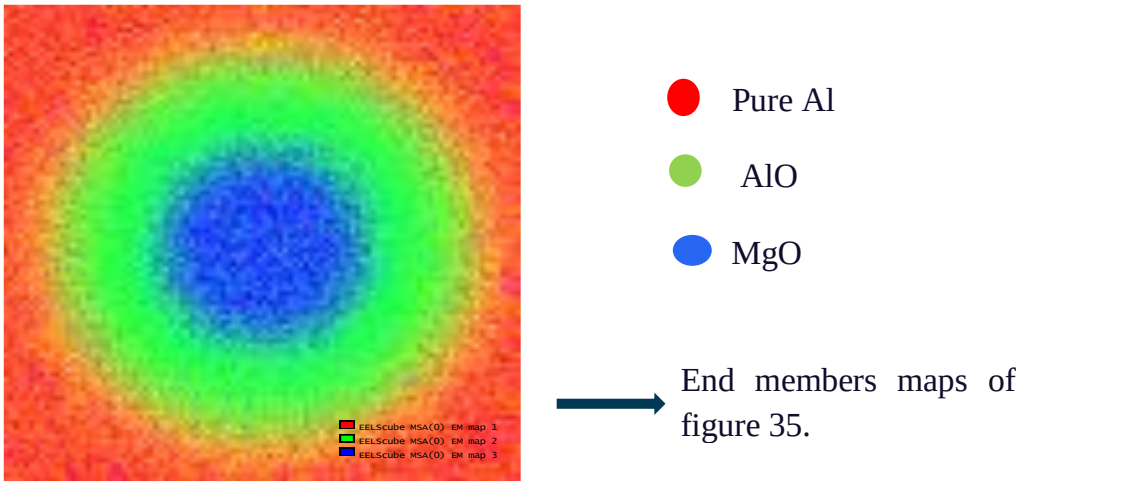


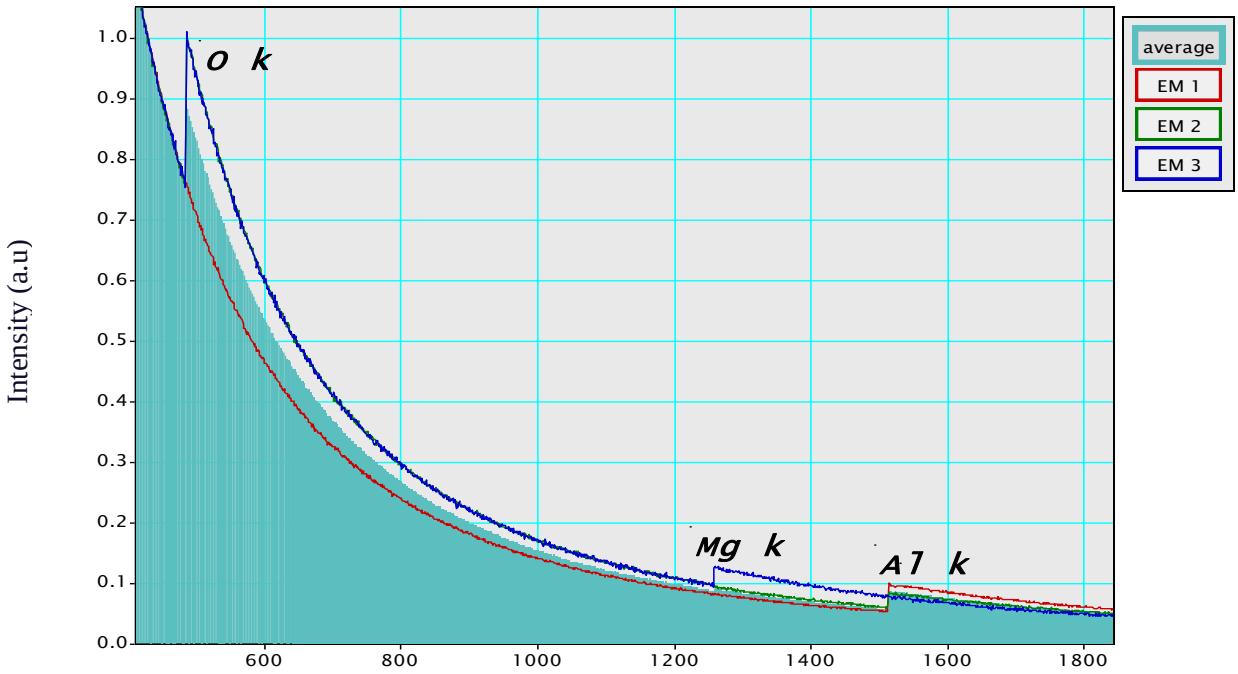


*Figure 35 End members representation of PCA1 and PCA 2*

## 4.2 Simulation of EDS data

EDS images are quite high noisy due to the continuous of Bremsstrahlung radiation in spectra and nonlinearity of data sets however, PCA is designed to model linear variabilities in high dimensional data. EDS data are treated with special effect of binning and then gaussian filter is applied. Binning is the merging of neighboring pixels into linear combination and the prescription of linear combination is called 'Kernel' or mask or filter. Binning in the order of two makes each pixel will be merged with 4 pixels making average mean spectrum so, binning should only be done if EDS SI is highly noisy and, the disadvantage of binning is the loss of original pixel data after binning where edge information of spectra can be lost. After binning the data set is subjected to Gaussian filtering to improve the signal to noise ratio which were lost in binning and even after applying gaussian filtering(Gss filtering) the atomic positions of elements are not visually improved. After application of PCA by selecting components with greater variances are selected for improvement of atomic maps.

### a) Strontium Titanate($SrTiO_3$) :

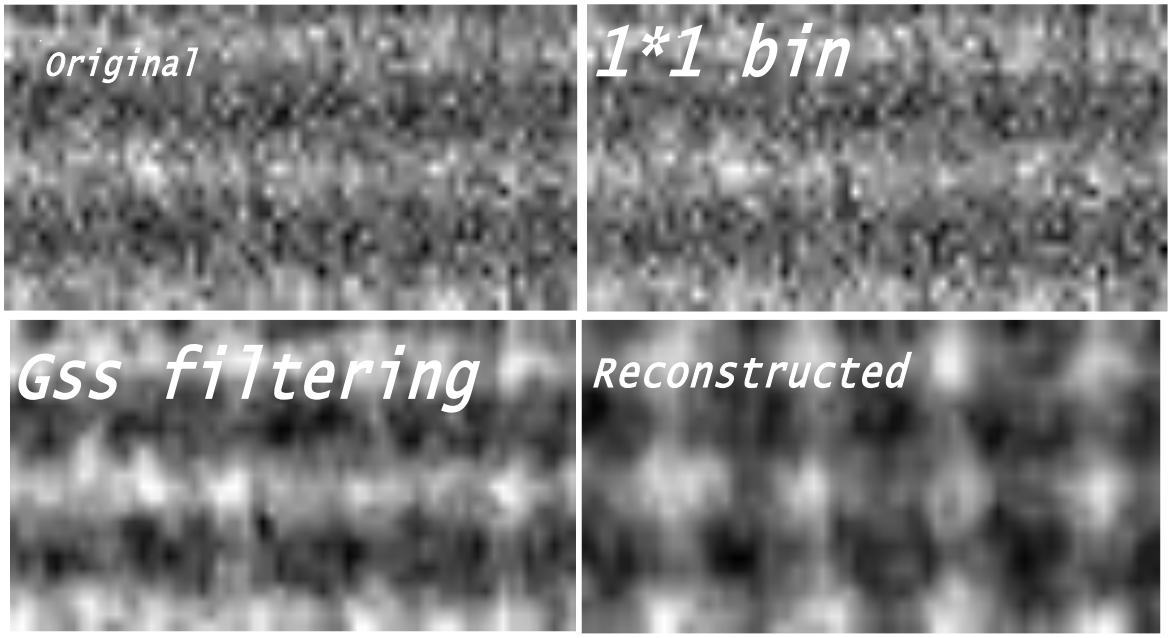


***Figure 36 Mean image (1) original data cube, (2) after binning the 1*1binning, (3) after the gaussian filtering + spatial filtering (4) PCA reconstructed atomic map.***

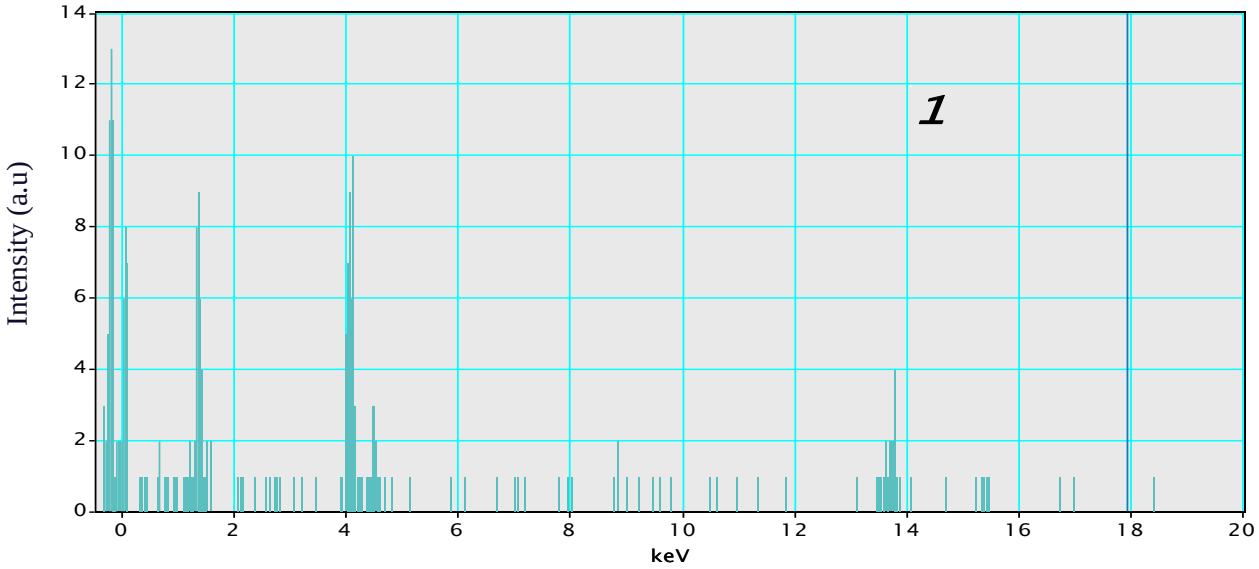

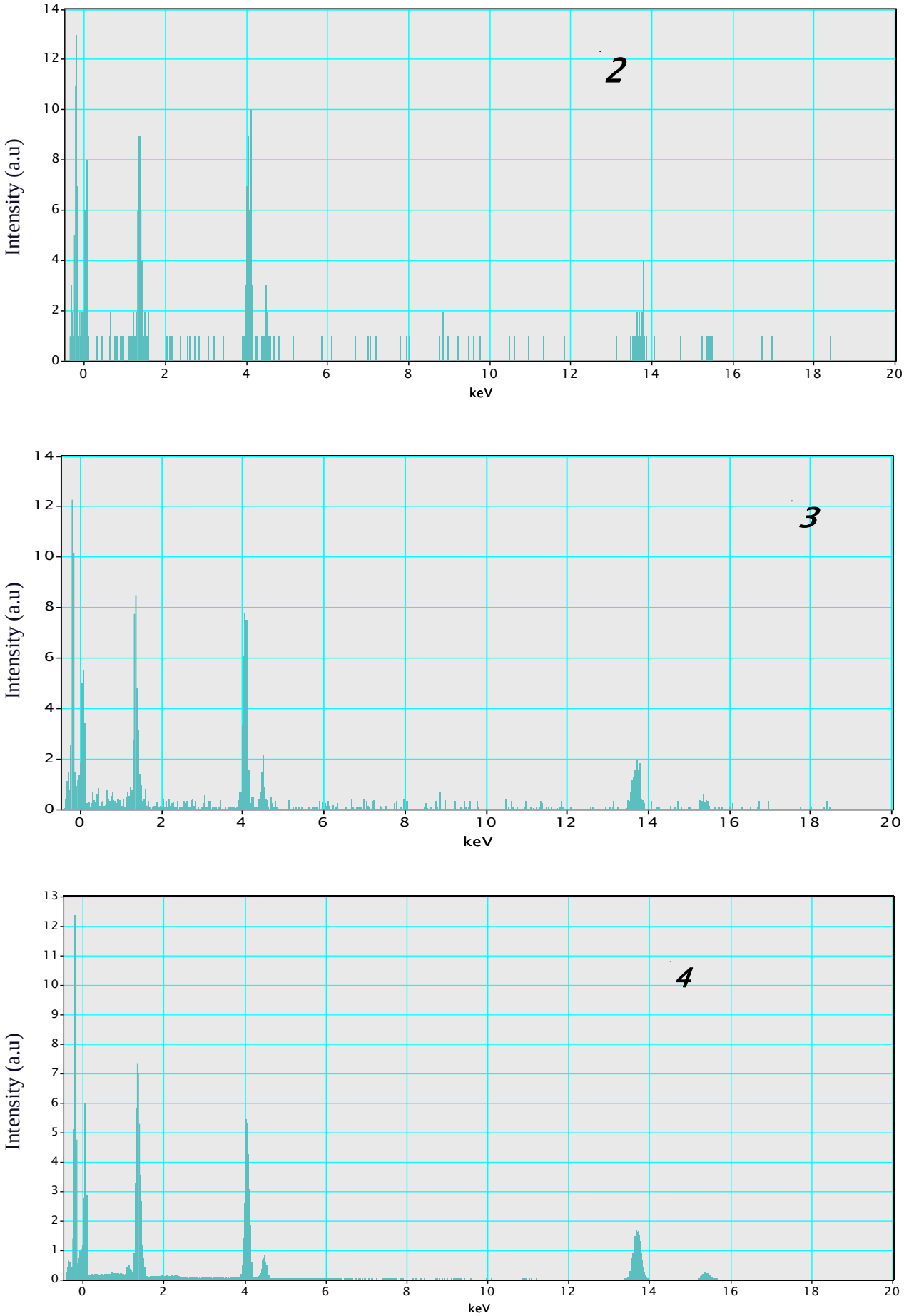


*Figure 37 Spectrums of fig. 36 corresponding Mean image (1) original data cube, (2) after binning the 1*1binning, (3) after the gaussian filtering + spatial filtering (4) PCA reconstructed atomic map*

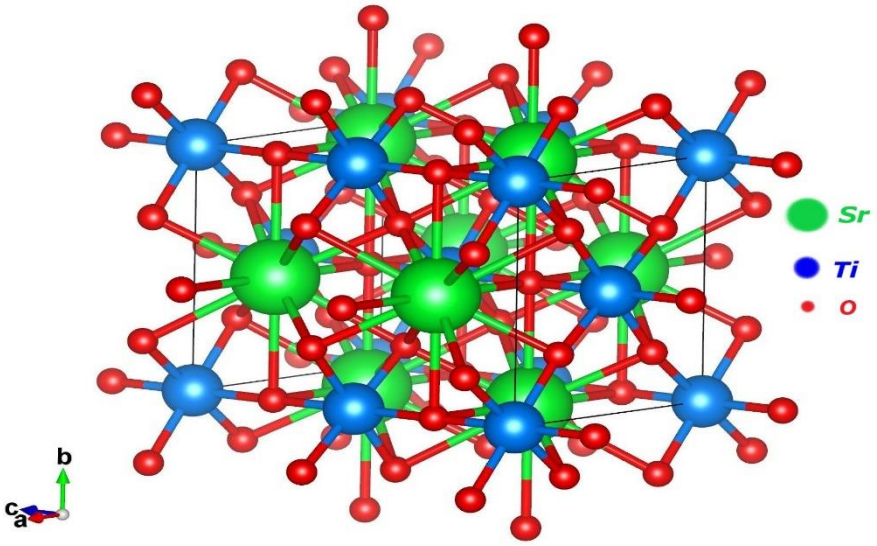


*Figure 38 Structure of $SrTiO_3$ modeled through VESTA software.*

*Figure 39 $SrTiO_3$ RGB composite atomic arrangement map.*

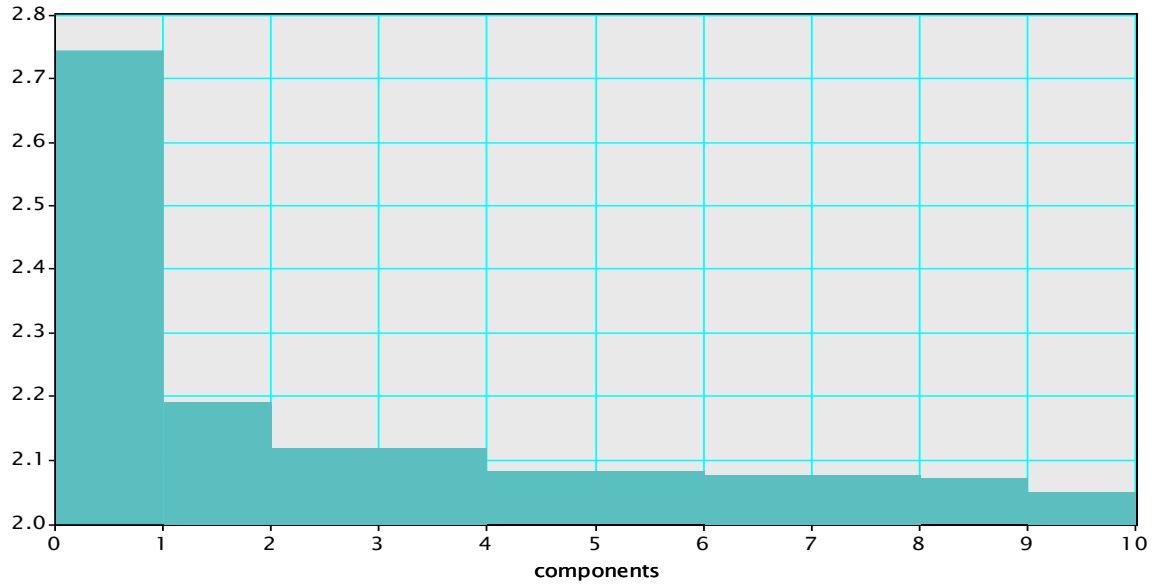


*Figure 40 Variance histogram of PCA 1 to 10 components where first two components exhibit greater variation and rest expose noise.*

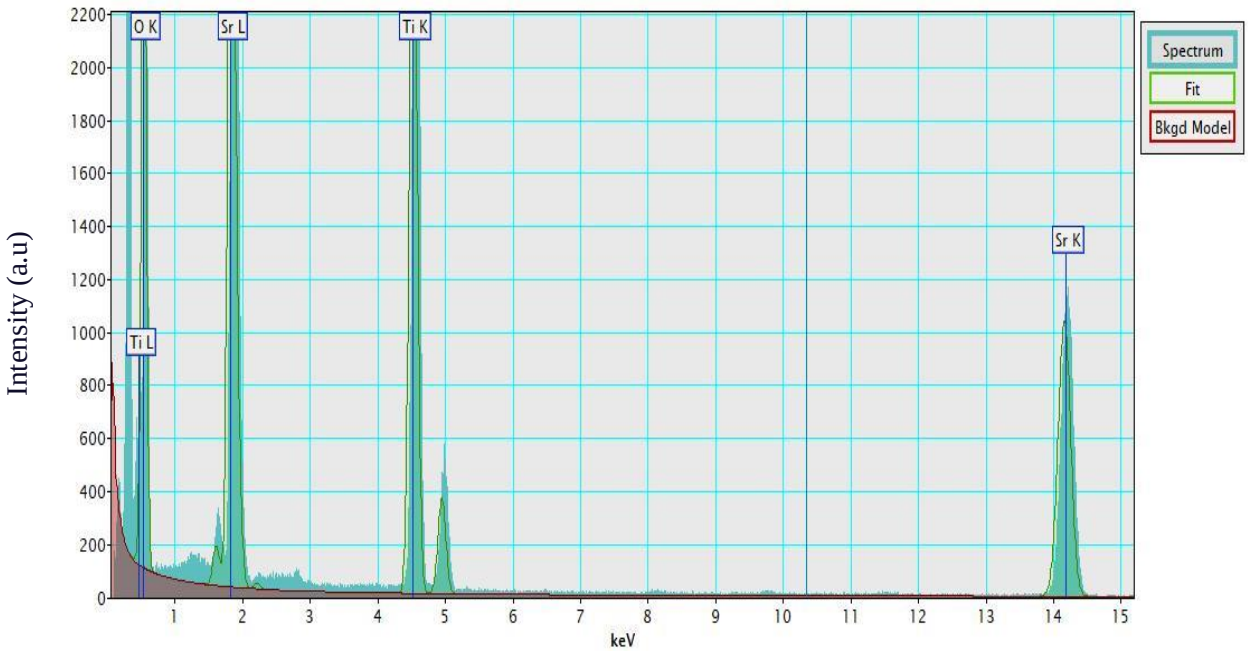


***Figure 41 Spectrum of Reconstructed image O-k at 0.52 KeV, Ti-k at 4.51 KeV and Sr-k at 14:16 KeV***

Application of binning and Kernel gaussian filtering has effectively reduced noise levels in case of EDS SI. From fig. 36 we can observe how significantly the atomic maps are improved with respect to spectrums in fig. 37. The accuracy and precision of PCA for high noisy spectrum imaging with linear projection of data sets are projected. From fig. 39 an RGB composite atomic map of SrTiO3.

b) Silica-Germanium (Si-Ge) :

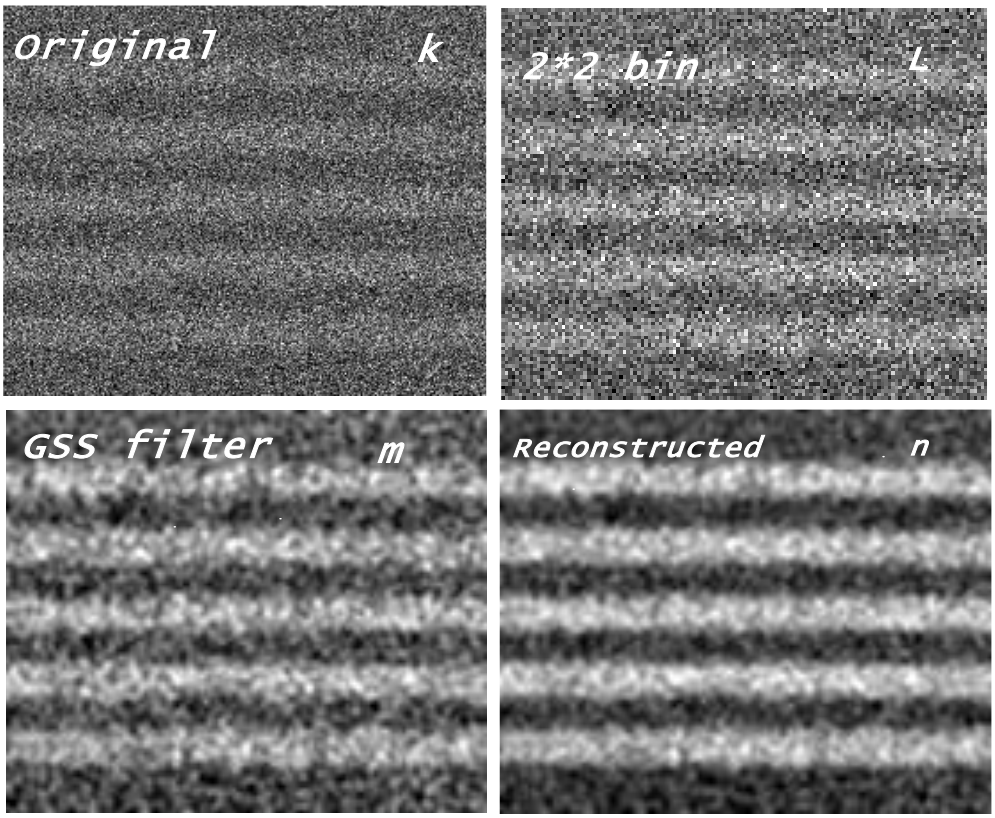


***Figure 42 Si-Ge EDS SI (k)-original data cube, (L)-after 2*2 binning, (m)-Gaussian filtering with spatial energy and (n)-Reconstructed data cube.***

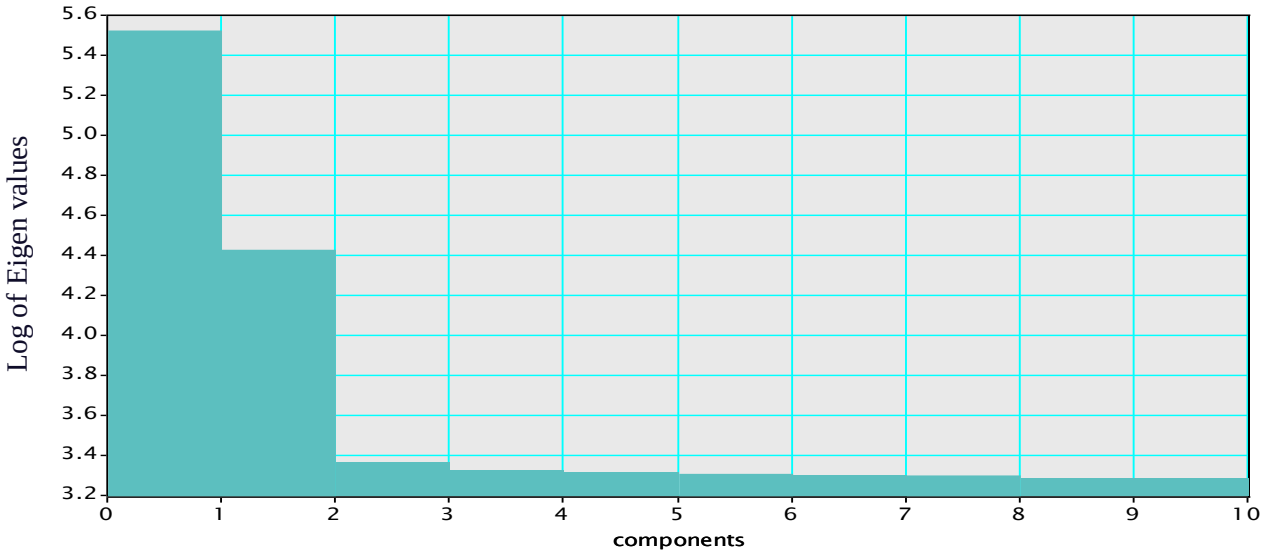


*Figure 43 PCA histogram variance showing only first two components having higher variation which are considered for reconstruction and rest of components are of noise.*

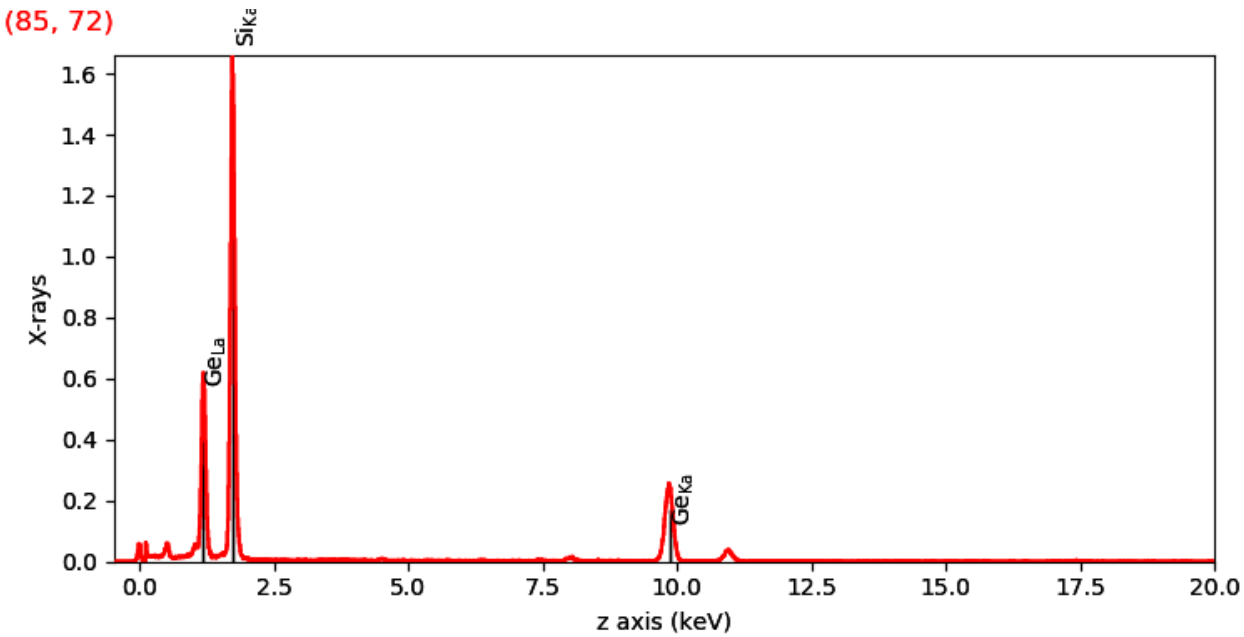


*Figure 44 Generated using Hyper spy Bundle tool showing EDS of Si-k shells and Ge-k, L shells.*

The model used for $SrTiO_3$ is used same for Si-Ge spectrum extractor shown in fig.44 with Si-k shell and Ge-k,l shells.

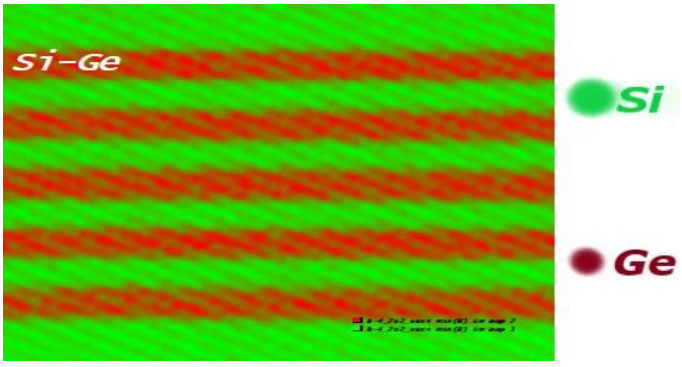


*Figure 45 Si-Ge layer by layer artifact composition map.*

## 5 Conclusion

From the results, PCA treatment for EELS data cube yielded accurate results and for EDS data we have to pretreat them with binning and gaussian filtering smoothing methods. The crucial factor for denoising spectrum is to consideration of principal components order which has the highest variation and the theoretical statement of retained principal components depend on the signal to noise ratio with the total number of pixels in SI. EELS spectra has better improvised chemical peaks when compared before and after PCA treatment and end members representing clear cut information of chemical maps of individual elements. In EDS we have extracted $SrTiO_3$ atomic arrangement maps and can improve more accurately with low filtering algorithms. In case of perovskites EELS spectra would be much more difficult to identify edges, which requires supervision. If the variation of principal components doesn't differ then the data in SI is having less pixels or inappropriate for PCA. As, PCA is having the capacity to deal with multi-dimensional data sets STEM imaging has broad application in the development of 4 dimensional data sets. While PCA cannot distinguish any factors about phonons in EEL spectrum but by using computational methods such as DFT and pseudopotential methods would calibrate phonons. Application of big data analysis methods for spectroscopy studies made easier for atomic studies.

## 6 Acknowledgements

The project is supported by department of Physics from 'Nano structuring-Nano Analytics-Photonic materials' working group at Universität Paderborn and the data used for simulation is obtained from University of Paderborn and Pavel Potapov's temdm.msa PCA plugin designed for digital micrograph.

## 7 References

[1] C. Barry Carter. David B. Williams, Transmission Electron Microscopy (A Textbook for Materials Science), Springer.

[2] Frank Krumeich, "Properties of Electrons, their Interactions With Matter and Applications in Electron Microscopy," ETH ZÜrich, ZÜrich.

[3] Nobuo Tanaka, Scanning Transmission Electron Microscopy of Nanomaterials (Basics of Imaging and Analysis), London: Imperial College Press.

[4] B.J, Inkson, "Scanning electron microscopy (SEM) and transmission electron microscopy (TEM) for materials characterization," in *"Materials Characterization Using Nondestructive Evaluation (NDE) Methods"*, 2016, pp. 17-43.

[5] Peter D. Nellist, Stephen J. Pennycook, Scanning Transmission Electron Microscopy Imaging and Analysis, Springer.

[6] F.Hofer, F.p Schmidt, W Grogger and G Kothleitner, "Fundamentals of electron energy-loss spectroscopy," in *IOP*, 2016.

[7] eels.info, Gatan Corporate, [Online]. Available: https://www.eels.info/about/overview. [Accessed on : 05/05/2019].

[8] Alex Williams, Neuronal blog, temDM, [Accessed on : 10/05/2019]. [Online].Available: http://alexhwilliams.info/itsneuronalblog/2016/03/27/pca/

[9] I.T, Jolliffe, Principal Component Analysis (A Text book for Multidimensional statistics), Berlin, Springer.

[10] Potapov pavel, "Why Principal Component Analysis of STEM spectrum-images results in “abstract”, uninterpretable loadings?", *Ultramicroscopy*, vol. 160, no. 0304-3991, pp. 192-212, 2016.

[11] M Watanabe, E okunishi, K Ishizuka, "Analysis of Spectrum-Imaging Datasets in Atomic-Resolution Electron Microscopy", *Microscopy and Analysis*, 2009.

[12] C. Ahn, Transmission Electron Energy Loss Spectrometry In Materials Science and The EELS Atlas, Weinheim: Wiley-VCH GmbH, 2004.

[13] Channing C.AHN, Peter Rez, "Inner shell edge profiles in electron energy loss spectroscopy", *Ultramicroscopy*, vol. 17, Issue-"0304-3991", pp. 105 - 115, 1985.

[14] J. S. Ramírez, "Big data analysis applied to EEL spectroscopy," Universitat de Barcelona, Barcelona.

[15] Paolo Longo, Pavel Potapov, "Enhancement of noisy EDX HRSTEM spectrum-images by combination of filtering and PCA", *Micron*, vol. 96, 2017.

[16] Francisco Javier de la Peña Manchón, "Advanced methods for Electron Energy Loss Spectroscopy core-loss analysis", Universite Paris-SUD11, Paris, 2010.

[17] G. Bertoni, J. Verbeeck, "Accuracy and precision in model based EELS quantification," *Ultramicroscopy*, vol. 108, Issue- "0304-3991", pp. 782 - 790, 2008.